University of Nairobi

School of Engineering

Billboard Measurements using Oblique UAV Images for Improved Revenue Collection

A Case Study of Nairobi City County.

BY

Hezron Seya Ndiege

F56/12421/2018

A Project submitted in partial fulfillment for the Degree of Master of Science in Geographic Information Systems in the Department of Geospatial and Space Technology of the University of Nairobi.

August, 2020

Declaration

I, Hezron Seya Ndiege, hereby declare that this project is my original work. To the best of my knowledge, the work presented here has not been presented for a degree in any other Institution of Higher Learning.

Hezron Seya Ndiege 21/08/2020

Name of student Date

This project has been submitted for examination with our approval as university supervisor(s).

Mr. B. M. Okumu …………………

Name of supervisor Date

Dedication

I dedicate this project to my father, who has taught me many valuable lessons about life and persistence, for his unwavering support and encouragement in pursuit of my Master's degree.

I also dedicate this project to my mother, who taught me no matter how hard a task may seem, it can always be accomplished one step at a time.

Finally, this dedication goes to my family, especially my two lovely daughters, Angel and Ayana. You're my biggest cheer leaders. May this be an inspiration to relentlessly pursue knowledge, become persons of value and achieve the fullness of your destinies.

Acknowledgement

My sincerest gratitude goes to the almighty God for the mental strength, good health and protection. It is by His grace that I made it this far. I'd also like to acknowledge and thank my Supervisor, Mr. B. M. Okumu, for his encouragement, support and counsel throughout this research project.

Special thanks to Mr. Fredrick Arthur Onyango for providing me with the base data captured using his UAV and technical advice in using Image processing software.
I'd also like to thank Mr. Savio Omalla and Ms. Irene Lwanga for their generosity and professional courtesy in assisting me during field data collection and providing a robotic total station for free!

I wish to thank my family as well for being understanding during the long hours spent on research, as well as my colleagues and classmates with whom I shared different concepts and ideologies with. Last but not least, I thank the Department of Geospatial and Space Technology (University of Nairobi), for equipping me with the skills and knowledge required to undertake this research.

Table of Contents

List of Tables

List of Figures

Abbreviations

AAT: Automatic Aerial Triangulation

AOI: Area of Interest

DEM: Digital Elevation Model

DSM: Digital Surface Model

DTM: Digital Terrain Model

GCP: Ground Control Point

GLONASS: Global Navigation Satellite System

GNSS: Global Navigation Satellite System

GPS: Global Positioning System

GSD: Ground Sampling Distance

HOT: Height of Target

KCAA: Kenya Civil Aviation Authority

LED: Light Emitting Diode

LIDAR: Light Detection and Ranging

OGC: Open Geospatial Consortium

OOH: Out of Home

PMVS: Patch Based Multi-View Stereo Software

RAM: Random Access Memory

RGB: Red, Blue and Green

RMS: Root Mean Square

RMSE: Root Mean Square Error

ROC: Remote Aircraft Operators Certificate

RTK: Real Time Kinematic

SfM: Structure from Motion

TLS: Terrestrial Laser Scanning

UAV: Unmanned Aerial Vehicle

UTM: Universal Transverse Mercator

VP: Validation Point

VT: Vertical Target

VTOL: Vertical Take-off and Landing

Abstract

Nairobi City County is one of the smallest yet most populous of the 47 counties in Kenya. Being one of the cornerstone counties of the economy of Kenya, its limited resources must be managed properly to guarantee sustainability. One of the major revenue streams of the county is Outdoor Advertising which currently rakes in an annual average of KS. 700 million against a potential of Ksh. 2 billion (Omulo, 2018). This means that revenue collection is not optimized and according to the county's Annual Development Plan 2020-2021, the county seeks to employ technology and expertise, especially from the private sector, to improve its revenue collection and compliance to by-laws.

This study therefore employs the use of Unmanned Aerial Vehicle (UAV) imagery and advanced Photogrammetric techniques to measure billboards for purposes of inventory keeping and monitoring. As was proven by the hypothesis, the process can be a cheaper and faster alternative to creating georeferenced 3D models, which have previously been a preserve of sophisticated and expensive methods like laser scanning. In the end, a 3D georeferenced render of the scenery was generated, with good planimetric and altimetry accuracies. Aerial oblique images were used to generate a dense point cloud by using an image matching algorithm that deduces the interior and exterior orientation parameters to reconstruct a georeferenced 3D model of the areas of interest.

The model was then used to accurately measure billboard dimensions, which is the basis for advertising rates. With this data, more informed revenue projections can be made and even help keep an inventory of the number of billboards and their usage along every stretch of the road within the city.

CHAPTER 1: INTRODUCTION

1.1 Background

Outdoor advertising is also referred to as out-of-home advertising (OOH) and involves the use of public places for marketing by means of media such as billboards and posters (Juntao Lai et al., 2017). In Kenya, it's a multi-million-shilling industry with many companies and Governmental organizations racing for public spaces to market their goods and services. Being a key element in revenue generation for many counties, outdoor advertisement needs to be regulated and managed to guarantee good revenue returns and an amicable business environment for all.

In Nairobi City County, Outdoor advertising is the fifth largest source of internal revenue (Omulo, 2018). However, according to the Nairobi City County Budget Review and Outlook paper (2019), the county has been on a downward spiral in terms of meeting set revenue targets. To this effect, the Nairobi City County Government launched tough measures to curb the loss of revenue and ensure compliance to regulations by assenting the Outdoor Advertising and Signage Control and Regulation Bill 2018. According to the County Annual Development Plan 2020/2021, collection from billboards can be improved by leveraging on the expertise of the private sector especially in monitoring. This will consequently necessitate introduction of innovative means of management and monitoring like the use of GIS technology and recent inventions like commercial Unmanned Aerial Vehicles (UAVs).

UAVs commonly known as Drones have had quite a huge impact in the consumer world. Since their emergence, they have had virtually limitless applications in various industries from the filming and entertainment industry to the medical field, and presently, as an alternative means of surveillance in the Geospatial field. Digital Photogrammetry traditionally used satellite images and orthophotos obtained using aeroplanes. Things have since shifted owing to the advancement in technology and subsequent launch of UAVs into the consumer market. Much as the platform has changed, the Photogrammetric principles remain the same as shall be elaborated in detail.

In this research project, the use of UAV imagery and Photogrammetric techniques were applied in rendering a 3D georeferenced model of road corridors in Nairobi for purposes of measuring billboards erected alongside major roads. This will not only help the county keep an inventory of the number of billboards and their usage, but also their exact dimensions, thereby giving an informed projection of expected revenue.

1.2 Problem Statement

Nairobi City County is grappling with inefficient revenue collection from Outdoor advertising. While growing consumerism has given rise to a large number of advertisements especially along major roads, this hasn't translated into a realisation of the optimal revenue potential. As illustrated in Figure 1.1 below, there has been a significant proliferation of billboards, especially along major roads like Mombasa road, Thika road, Lang'ata road and Waiyaki way (Wako, 2019).

Figure 1. 1: A road section in Nairobi with several billboards erected.

(Image source : http://expatprint.co.ke/wordpress/)

According to the Nairobi City County Budget Review and Outlook Paper (2019), the exact figure raised by billboards and adverts was Ksh. 797 million against a target of Ksh 1 billion in the financial year 2018/2019. This was a Ksh. 203 million shortfall and 20.3% deviation from the target.

The report attributes the decline to non-adherence to regulations and inadequate enforcement of county by-laws. In addition, the Outdoors Advertisers Association of Kenya also say that it costs a minimum of Ksh. 160,000 per month to erect a 12 by 10-meter billboard, which is the most common billboard in major cities in Kenya. This means that advertising doesn't come cheap but somehow, this glam picture doesn't reflect on the financial statements in City Hall.

By ratifying the Outdoor Advertising and Signage Control and Regulation Bill 2018, the Nairobi City County Government seeks to impose more stringent rules and regulations that will guarantee sustainable outdoor advertising and improved revenue collection. As seen in Figure 1.2 below, the crackdown on illegally erected billboards had already started by early last year. The new policies also plan to leverage on the private sector in employing technology to help in monitoring assets and coming up with innovative means of revenue generation (Draft Annual Development Plan 2020/2021).

Figure 1. 2: *An illegal billboard being brought down on Uhuru Highway on March 5, 2019.*

(Image source: Nation Media Group)

Keeping a good inventory of billboards erected within the County would be a good start in improving asset monitoring. In light of improving revenue collection, this project therefore seeks to provide a cheaper and faster means of monitoring and keeping an inventory of billboards by creating a 3D model using UAV imagery, from which the actual number and dimensions of billboards can be measured.

1.3 Objectives

Main Objective

The main objective of this study is to determine the reliability of using UAV imagery to accurately measure billboards, for purposes of improved revenue collection. Since the advertising rates are based on the size and area of billboards, reliable measurements provide a good framework for revenue projections and monitoring.

Specific Objectives

The specific objectives of the study entail:

i) Generate a 3D model of billboards from acquired UAV imagery
ii) Assess the geometrical accuracy of the 3D model generated.
iii) Acquire billboard dimensions from the 3D render
iv) Validate the accuracy of acquired dimensions by comparison with measurements taken by traditional means (Total station)

1.4 Justification for the Study

Nairobi residents and the general citizenry deserve some level of accountability from the county. Every year consolidated financial statements and budgetary reports are released to the public, and more often than not, a significant amount of money is left unaccounted for owing to reported fiscal malpractices and weak enforcement that result into loss of revenue.

Many problems Nairobi residents face require practical solutions that can only be implemented and executed when the right technology is employed by the right people.

This project is therefore instrumental in ensuring one of the major revenue streams of the Nairobi City County Government is fully exploited and the revenue collection success rate raised to at least

80% of its potential. The approach used to address this problem entails the use of UAV imagery to reconstruct a georeferenced 3D scenery from which accurate billboard measurements can be taken. If proven reliable, this will be a very cheap and fast means of monitoring billboards and projecting expected revenue returns. Traditional methods of measuring erected billboards will most certainly be more expensive and time consuming in the long run.

The Nairobi City County Government the other 46 Counties for that matter, may find this report invaluable, as it will highlight the quickest, cheapest and most practical way of estimating the potential revenue from outdoor advertisements while ensuring compliance to the advertisement and signage rules.

1.5 Scope of work

The county's Outdoor Advertising and Signage Policy encompasses many advertising signs such as clock advertisements, billboards, wall brandings, and sign boards among many others. This research, however, was confined to billboards only to demonstrate its feasibility.

Owing to the previous inexistence of a legal framework governing the usage of UAVs in Kenya, this study did not require acquisition of UAV imagery. UAV images that were previously taken before the cease order given by the Kenya Civil Aviation Authority (KCAA) in 2015, were used.

However, on 30th March 2020, parliament approved and ratified the Civil Aviation (Unmanned Aircraft Systems) Regulations, 2020. This meant that the ban on flying drones was lifted albeit under strict guidelines.

The study area was also confined to Nairobi City County. Due to the vast expanse of the road network and billboard distribution within Nairobi, only a section of Thika road (near Muthaiga roundabout) for which reliable data was available, was used to conduct the study. The study will also focus on the revenue aspect of billboard advertisements only, and not their legality, requirements or prohibitions which are diverse.

CHAPTER 2: LITERATURE REVIEW

2.1 Current Laws Governing Billboard Advertisements in Nairobi

Outdoor advertisement in Nairobi is one of the main internal revenue sources in the county. Being an integral part of the county's revenue streams, its proper management is crucial in ensuring it remains profitable and sustainable. To support this endeavour, the program budget estimates for Outdoor Advertisement automation and mapping of High Impact Advertisement was set at Ksh. 15 million for financial year 2020/2021 (Draft County Annual Development Plan, 2020-2021)

The recently assented Outdoor Advertising and Signage Control and Regulation Bill 2018 outlines the general requirements, exceptions and prohibitions for advertising signs. These include signs on residential buildings, signs suspended under verandas or canopies, screens for sky designs, painted advertisements and transit advertisements among many others.

The new law highlights the regulations on displayed messages, design issues such as sign-clutter controls, costs of removal and storage, protrusion of advertisement structures on road reserves, offences and penalties.

The main aim of the new regulations is to increase and enhance revenue collection, ensure sustainable outdoor advertisement by controlling spacing between billboards, reducing street clutter and the number of signposts placed along roads. These include the lit-box adverts on streetlight poles. Of utmost importance are the new rates for billboard advertisement as stipulated in the amended Nairobi City Council Finance Act 2015. Table 2.1 below summaries the comparison between the old and new advertising rates.

Table 2. 1: A comparison of previous and current billboard rates in Nairobi City County

Previous Rates	New Rates
Application fee: Ksh. 10,000	Application fee: Ksh. 14,000
First 3 square meters or part thereof: Ksh. 36,400	First 3 square meters or part thereof: Ksh. 36,400
Additional area per square meter or part thereof: Ksh. 3000 p. a	Additional area per square meter or part thereof: Ksh. 5,733 p. a

2.1.1 Sustainable Outdoor Advertising

According to Garcia Jennifer (2018), sustainable outdoor advertising entails guaranteeing the survival of commercial communication, environmental responsibility and a systematic approach to advertisement that ensures seamless integration with the architecture, urban and social setup of a city.

If not put in check, outdoor advertisement can result into disastrous effects to the environment owing to information saturation (clutter) and even toxic chemicals that might have been used in the advertising material. Regulation is therefore needed to regulate the use of materials and display of advertisements. Digital outdoor advertisements are considered more environment friendly than the typical canvas or plastic ads frequently used.

2.1.2 Characteristics of Sustainable Outdoor Advertising

Rodriguez and Alfaro (2008) attempted to outline the characteristics of suitable outdoor advertisements. According to their publication, sustainable outdoor advertisement consists of five main elements:

- Openness and sensitivity to the environment; where aesthetics is considered (i.e. design, shape and climatic conditions of a city)
- Creation of value; where the information must contain a social function
- Long-term consideration; where the design should be able to withstand the weather elements
- Innovative capacity; where the technology should be adaptable, e.g. the use of transparent digital screens and LED lights that work beyond 60° Celsius
- Sense of community; where the advertisements portray a certain cultural or symbolic function of the society or reflect their habits and customs.

Ultimately speaking, advertisements should not only benefit the company that pays for it, but also the society to which it is directed to (Aznar and Catalan, 2000)

2.2 Current Laws Governing Use of UAVs in Kenya

The law in Kenya had previously been silent on the usage of UAVs until their prevalent use in early 2015. According to a publication by Derrik Koome (2019), there were no restrictions prior to the year 2015, forcing the Kenya Civil Aviation Authority (KCAA) to issue a cease and desist order until a legal framework governing the use of drones is drafted. In 2016, stakeholders met with KCAA and drafted some regulations, which were later presented to the National Security Advisory Committee for ratification.

On February 2017, the president assented to the draft policy pending parliamentary review. However, the draft policy was shot down in parliament with members citing lack of adequate stakeholder involvement and inconsistencies in application of fines and penalties. This sent KCAA back to the drawing board where the Authority drafted yet another set of regulations by late 2019, awaiting presentation to the parliamentary review committee.

In a publication by Eunniah Mbabazi (2020), the National Assembly finally approved the draft Civil Aviation Unmanned Aircraft Systems Regulations 2019 for commercial and recreational purposes, under strict oversight by the Kenya Civil Aviation Authority.

A summary of the main policies and regulations contained in the Civil Aviation (Unmanned Aircraft Systems) Regulations 2020 include:

i. UAVs are categorized as Low Risk (Category A, Medium Risk (Category B) and High Risk (Category C) based on the risk they pose on safety of individuals and national security.
ii. A person shall not import any UAV without permission issued by the Authority
iii. A person shall be required to register their UAVs and obtain a certificate of registration from the Authority in accordance with the categories of operations.
iv. In order to be eligible for ownership, a person must be a Kenyan citizen of at least 18 years of age, a corporate body or the national/county government.
v. To operate a UAV for commercial ventures, reward or hire, a person must obtain a Remote Aircraft Operators Certificate (ROC) at least 90 days before the date of intended operation.
vi. A person shall not operate a UAV 400meters below ground level or within 50 meters from any person, vessel, vehicle or structure

vii. A person shall not operate a UAV over a public road, along the length of a public road, or at a distance of less than 50 unless express permission is granted by the Authority

viii. A person shall not operate within 10 kilometres from an airport or landing/take-off zone

ix. Non-compliance attracts a fine not exceeding Ksh. 2 million or imprisonment for a term not exceeding 3 years or both.

These regulations had been in assessment for a very long time but finally, businesses and individuals can buy and operate UAVs without fear of breaking the law. This is critical, especially for businesses that fly drones for general digital content creation, mapping and even rescue missions. According to Eunniah Mbabazi (2020), it is projected that East Africa will generate revenues well over $150 million in the next 2-3 years from drone operations.

2.3 3-D Mapping and the Photogrammetric Workflow

Advancements in computational mathematics and image matching algorithms have enabled even non-metric cameras to be used in conjunction with UAVs to create 3-D models of scenery. According to Montgomery and Strecha (2015), Nadir and Oblique images are commonly used for model creation, but high-resolution terrestrial images can also be employed for this purpose. Similar image points (Tie Points) are used in conjunction with Ground Control Points (GCPs) to ensure a project is georeferenced and a dense point cloud generated.

Dense point clouds used to be acquired using expensive laser scanners. This has since changed with the advent of technology known as Structure-from-Motion (SfM), which is automated and has revolutionized Photogrammetric image processing. It’s main advantage over laser scanning is its high speed of data acquisition, better 3D texture in modelling and close-range image acquisition capabilities from many angles.

According to Remondino et al. (2011), the basic photogrammetric workflow involves three major sequential steps:

i. Flight Planning
ii. Camera Calibration and Image Triangulation
iii. Surface Reconstruction and Feature Extraction

Flight Planning

This is usually done before going to the field. It involves defining the Area of Interest (AOI), required ground sampling distance (GSD), knowing the intrinsic parameters of the mounted camera and computing the perspective centre. Advanced software is used to come up with the flight paths across the Area of Interest. Usually, images are acquired through computed waypoints in advanced systems while in low-cost systems, the images are acquired through a scheduled interval. Figure 2.1 below illustrates the flight paths generated using waypoints and digital markers. The intrinsic camera parameters are used to fix the image scale, focal length and flying height while the perspective centre computed is used for fixing the longitudinal and transverse overlaps. Take-off and landing operations usually depend on the type of drone used. Flight is then monitored using a control station showing real time flight data such as speed, altitude, camera position and battery status among many other on-screen statistics.

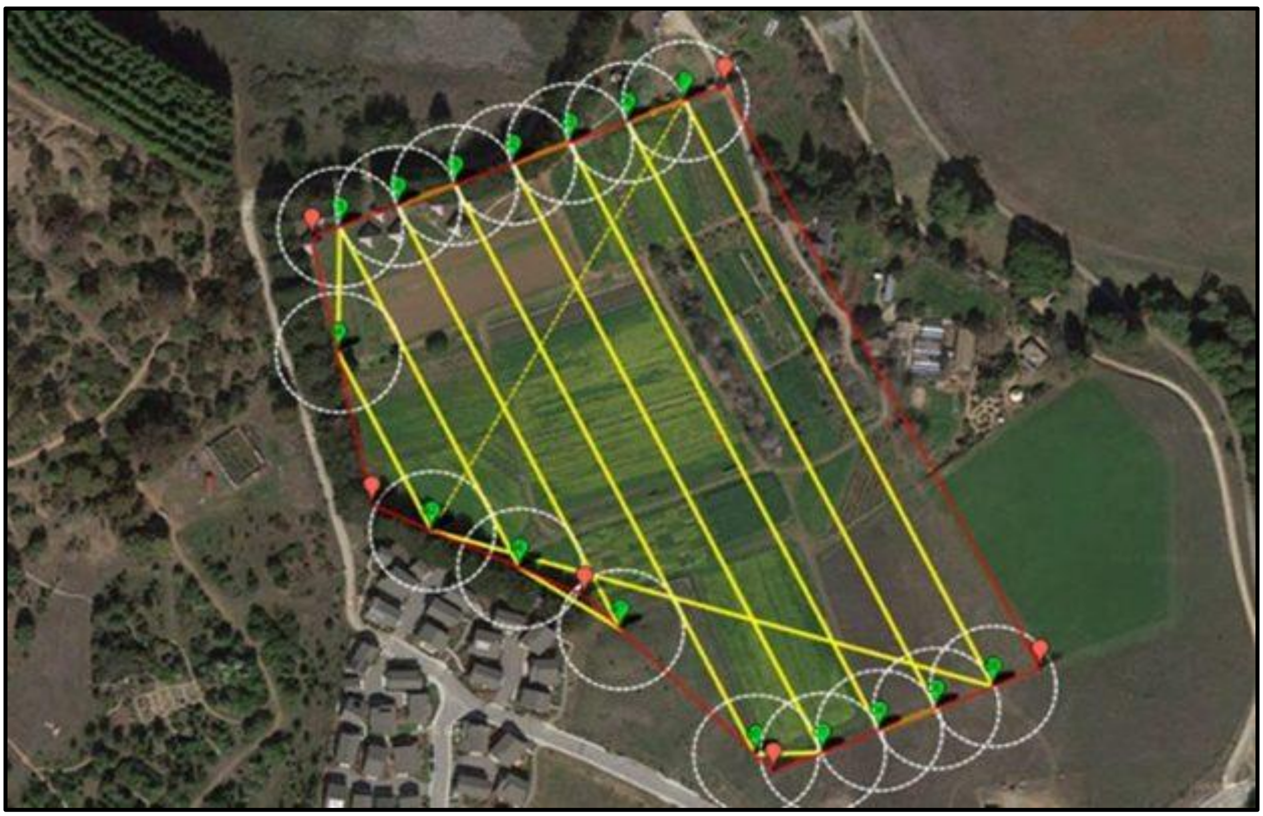

Figure 2. 1: UAV flight plan

Image source: https://www.ee.co.za/article/using-drones-map-land-ownership-kenya.html

Camera Calibration & Image Triangulation

After launching the platform and acquiring as many images as required, camera calibration and image triangulation is then performed to facilitate the metric reconstruction. These processes should be preferably done separately since they require different block geometries to be optimised (Remondino and Fraser, 2006). However, many applications perform the two operations simultaneously by a self-calibrating bundle adjustment. Bundle adjustment generally computes the camera poses and altitudes from the approximated exterior orientation parameters (Eisenbeiss, 2008). Exterior orientation parameters refer to the coordinates of the camera's focal point (x, y, z) measured in a right-handed mapping system and the plenary rotational angles omega, kappa and phi, that define the position and orientation of the camera in space when the image was taken (Wolf, 2000). The intrinsic parameters are assumed to be constant for all images if the same camera is used under the same condition.

Self-calibrating bundle adjustment requires extraction of common features that are visible from as many images as possible to facilitate automatic aerial triangulation (AAT). In theory, bundle adjustment allows for absolute orientation of an unlimited number of photographs all at once using at least three GCPs (Tanguay, 2019) as illustrated in Figure 2.2 below. However, their relative orientation must first be established using common points visible in two or more images (tie points).

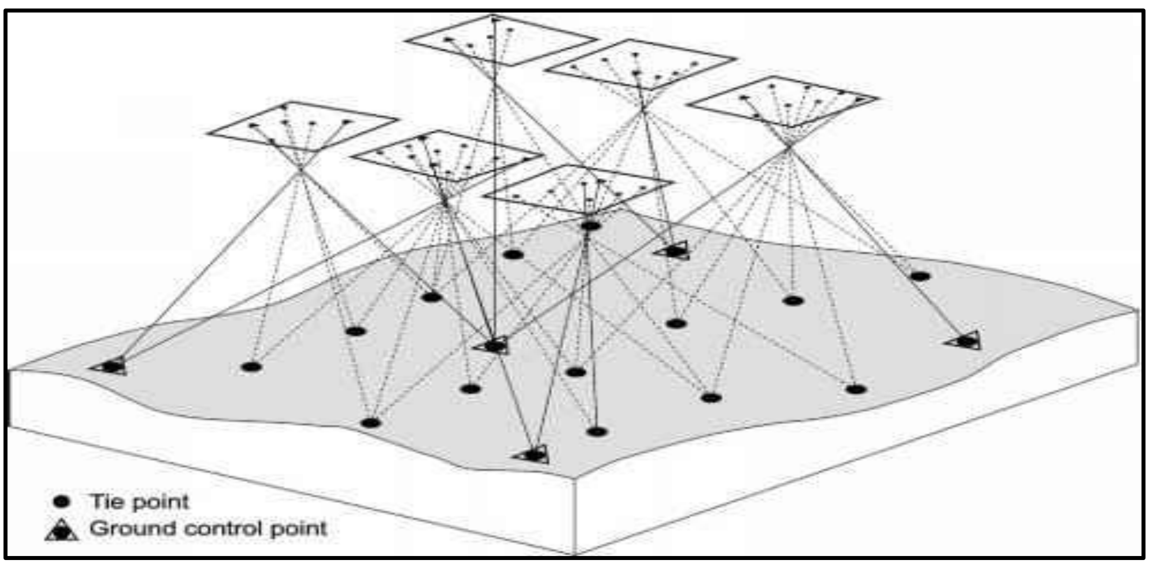

Figure 2. 2: Principle of bundle adjustment.

Image source: https://www.tanguayphotomag.biz

The procedures for extraction of both consistent and redundant tie points from marker less close-range images have been automated and incorporated in both commercial and opensource software. The in-built GNSS data helps in automated tie-point extraction which essentially allows for direct georeferencing of the images albeit with low accuracies. For very accurate georeferencing, measurement of ground control points (GCPs) is required. l

Surface Reconstruction and Feature Extraction

Once the images are oriented, the next steps involve surface reconstruction and feature extraction. From the exterior orientation parameters and camera calibration parameters, a scene can be automatically generated by an image-matching algorithm or by interactive feature extraction. Powerful image matching algorithms generate a dense 3D point cloud with sufficient resolution to describe the object surface and discontinuities as illustrated in Figure 2.3 below.0

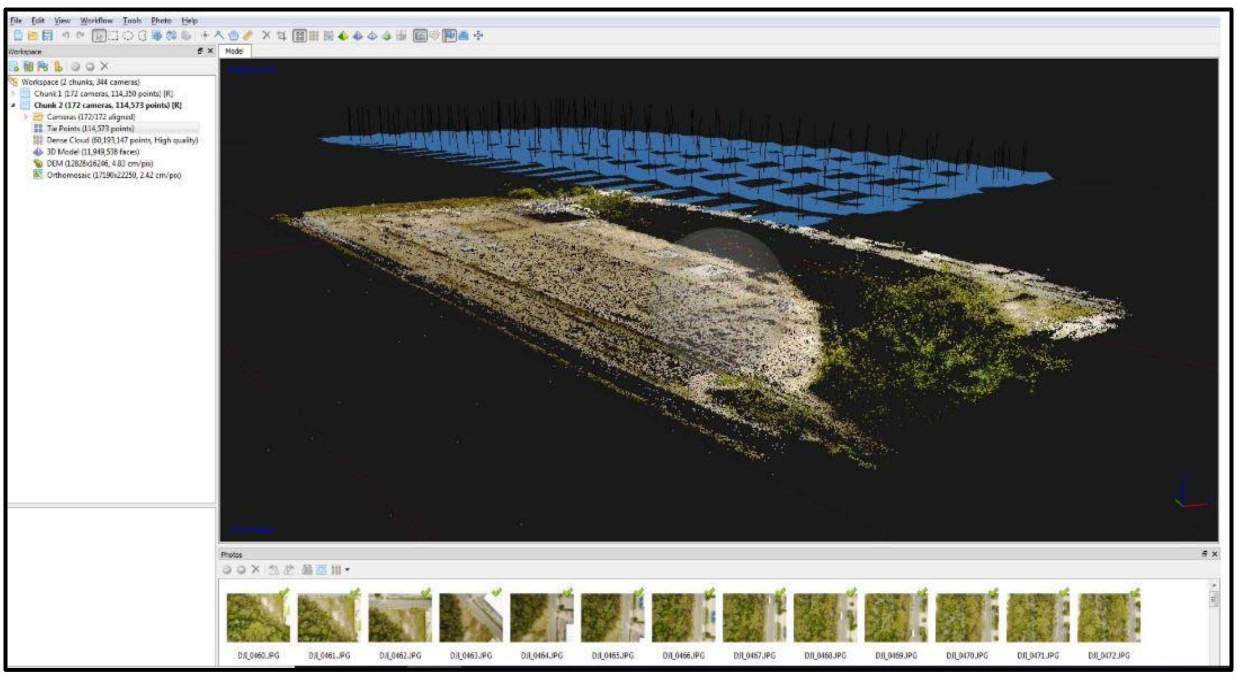

Figure 2. 3: Dense point cloud generated using Agisoft Photoscan

Image source: www.droneace.com

Interactive feature extraction results into a sparse point cloud which still require masking and editing to derive an accurate 3D render while the automated process results into a dense point cloud (Digital Surface Model) which has to be interpolated or simplified then textured to give a photorealistic visualization (Seitz et al., 2006).

State-of-the-art image matching techniques include:

1. Multi-image matching technique based on the semi-global matching algorithm
2. Patch-based methods
3. Optimal flow algorithms

The last two have been implemented in opensource software packages such as PMVS (Patch-based Multi-view Stereo Software) and MicMac

2.3.1 Structure from Motion Photogrammetric Principle

Structure from Motion (SfM) is a technique in which a 3D scene is reconstructed by estimating the camera parameters from camera motion from a sequence of 2D images taken around the scene with a moving camera as illustrated in Figure 2.4 below. Common feature points from multiple images are detected using an algorithm and used to reconstruct their movement in space. Using this information, the locations of those points are calculated and rendered as a 3D point cloud (Theia-sfm.org, 2020)

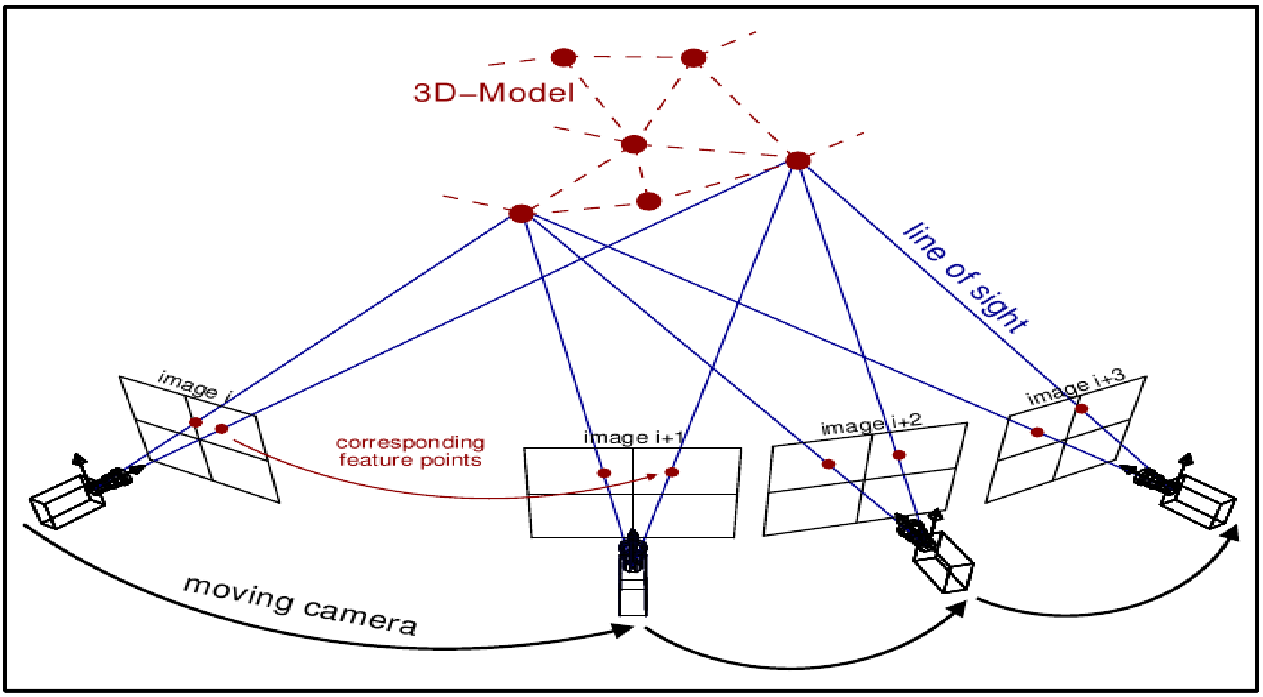

Figure 2. 4: Structure from Motion (SfM) photogrammetric principle.

(Image source: Theia-sfm.org (2020)

Typical uses of this technology range from reconstruction of surfaces for geomorphological analysis to disaster management and infrastructural inspection.

2.3.2 3-D Model Accuracy Evaluation

The accuracy of the resultant 3D model depends on certain Photogrammetric parameters which include (Montgomery and Strecha, 2015):

i. Angle formed between homologous rays (the greater the angle, the greater the accuracy)
ii. Measurement of GCPs
iii. Method used to estimate camera calibration parameters (in the lab or during post-processing)
iv. Flight parameters (altitude, image overlap and sensor resolution)

Basic accuracy evaluation procedures involve analysing residuals of the bundle adjustments. This is done by computing the Root Mean Square errors of the residues and is more often than not an automatic process where the software used returns a report after processing. In order to generate a good 3D georeferenced model, the GCPs should preferably be at the edge of the study area to ensure a well-rounded configuration for reprojection. It is worth noting that the quality of the 3D render may at times vary depending on the software used in modelling.

2.4 3-D Modelling software

Commercial Software

There are many software packages available for 3D image processing and mapping. According to (Thedroneu.com, 2020), the most common commercial software includes:

a) Pix4D
b) DroneDeploy
c) Agisoft Photoscan
d) RealCapture
e) Autodesk Recap
f) Photomodeller

Free and Opensource Software

Free and opensource software on the other hand include (Ubel. 2020):

a) ColMap
b) Meshroom
c) MicMac
d) Regard3D
e) OpenMVG
f) WebODM

Opensource software are however greatly limited in terms of functionality, output format options and support.

2.5 Similar Research

Research studies that have employed similar technology and concepts include publications titled:

i. Using UAVs for High Resolution Reconstruction of Topology (Mancini et al., 2013);
ii. High-Resolution Mapping Based on UAVs to Capture Paleoseismic Offsets (Gao et al., 2017) and;
iii. Estimating Tree Heights with Images from UAV (Birdal et al., 2017)

2.5.1 Using UAVs for High Resolution Reconstruction of Topography

This study was carried out in a beach dune system located in Ravenna (Italy) on the North Adriatic coast. The research combined the utility of Structure from Motion (SfM) technology and low altitude UAV imagery. The quality of the UAV data was then evaluated by comparing it to a point cloud generated using a Terrestrial Laser Scanning (TLS) system. The average vertical differences were found to be 0.05m with an RMS of 0.19m. For further geomorphological analysis, a multi-temporal surface analysis had to be carried out where interpolation became necessary. The vertical absolute accuracies of the DSMs generated using UAV imagery and TLS point clouds were compared to a GNSS survey, resulting into sub-centimetre differences with an RMS of 0.011m

The methodology involved a networked RTK survey, TLS and UAV flight performed on 27th May 2013. Using a GNSS-RTK dual frequency Topcon, the survey resulted into RMS values of 0.018m and 0.029m for horizontal and vertical accuracies. As shown in Figure 2.5 below, GCPs obtained were to be used as reference for bundle adjustment, Validation Points (VP) as reference for UAV validation and Vertical Targets (VT) for georeferencing the TLS point cloud.

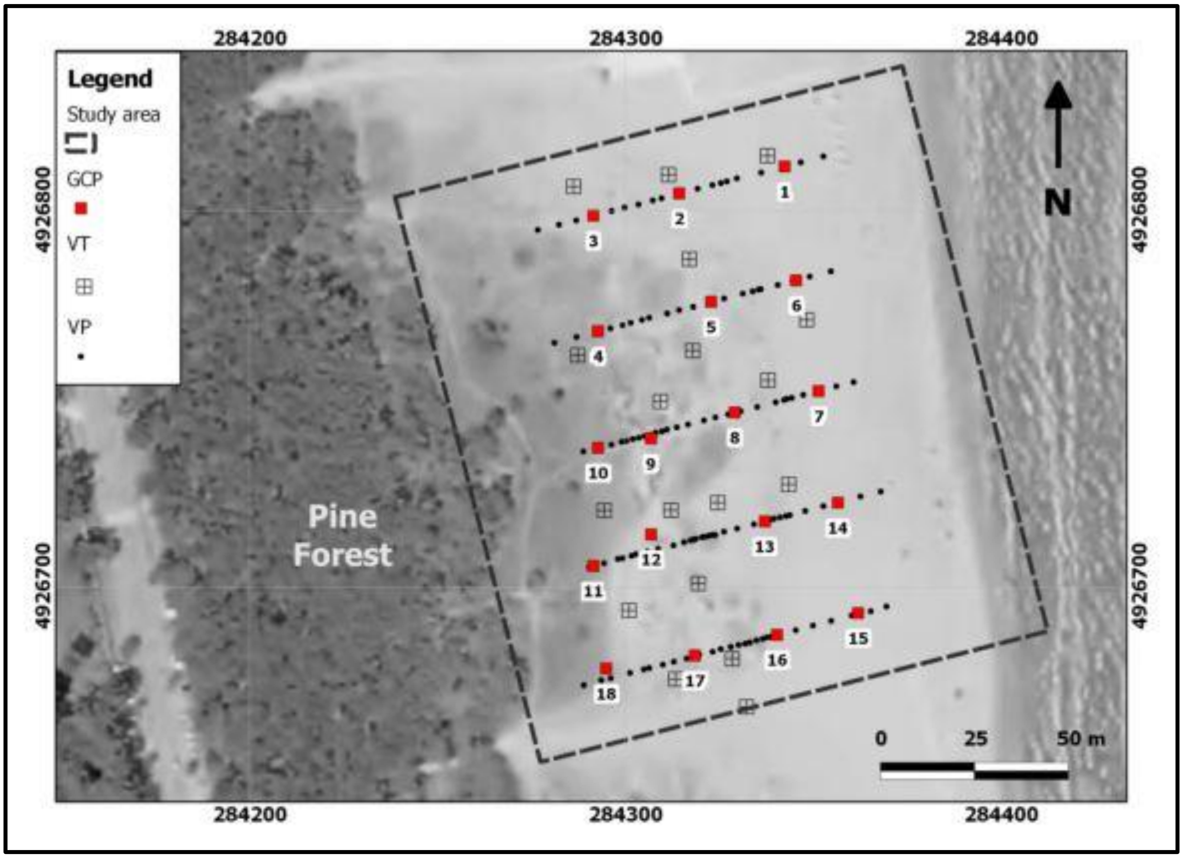

Figure 2. 5: Technical specification and survey of the Study Area

Image source : (Mancini et al., 2013)

After the flight planning, a VTOL (Vertical Take-Off and Landing) hexacopter with a calibrated Canon EOS Model 550D Camera was used to obtain 550 images, with a ground resolution of 0.06m/pixel at a 40meter flying height. The TLS survey was then done using a CAM2 Focus3D scanning system that took a total of 18 scans with a point resolution of 7.7mm resulting into a point cloud with 115 million points, which was then georeferenced using 19 vertical targets established in the GNSS survey to make a DSM.

The processing software used was Photoscan (by Agisoft). Generally, three highly automated steps were carried out by the software:

i. Image alignment, where the SfM algorithm was used to generate a dense point cloud from the UAV imagery and validated with GCPs acquired from the GNSS survey. 10 uniformly distributed GCPs were used for the bundle adjustment.
ii. Pixel-based stereo reconstruction using the aligned dataset to come up with a mesh of triangulated points
iii. Texturing applied to the mesh to obtain a continuous DSM. This automated process requires high computational powers that typically depend on the available RAM of the computer used.

The spatial error between the DSMs generated using UAV imagery and TLS was obtained by subtracting the UAV elevation from the TLS elevation and rendering the difference as a color-coded surface. This is illustrated in Figure 2.6. Below:

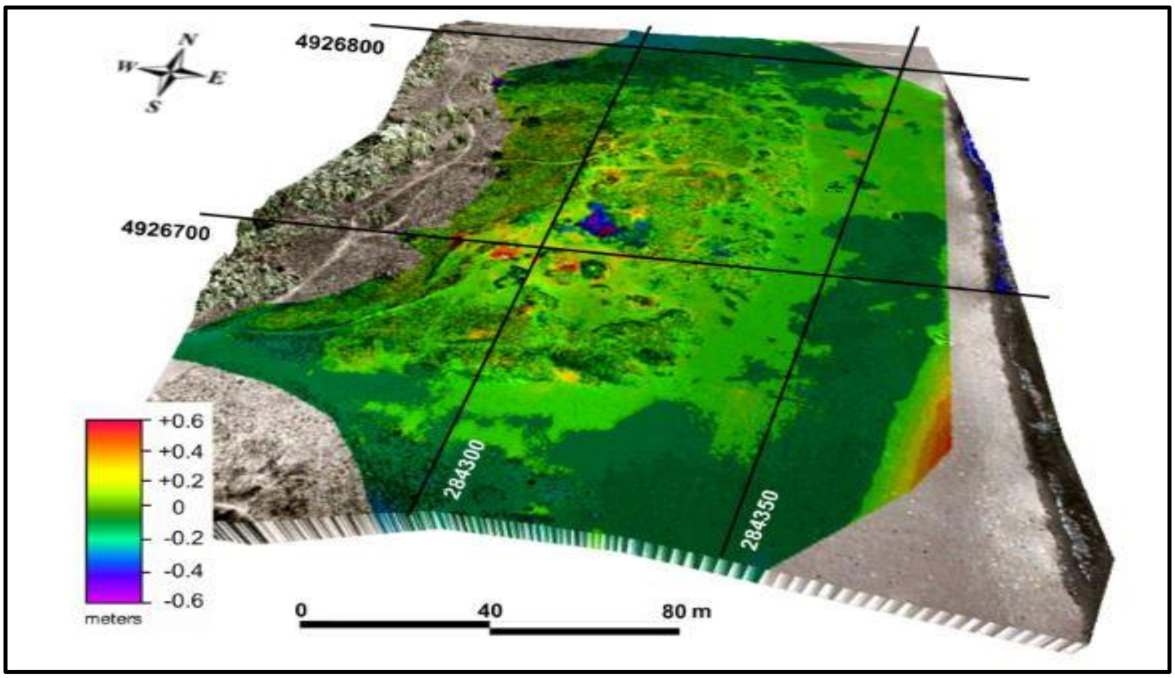

Figure 2. 6: Spatial error distribution between the DSM created by TLS and UAV imagery

Image source : (Mancini et al., 2013)

As was seen in the results above, the elevation differences were almost zero for most parts of the study area (green areas) leading to the conclusion that UAV and TLS generate high resolution DSMs with a good level of accuracies with respect to GNSS points. Larger values were only encountered in areas where there was a sudden change in topography. It was also concluded that TLS is two to three times more expensive than UAV surface reconstruction. A large number of redundant images also guarantees success in the automated process of point matching.

2.5.2 High-Resolution Mapping Based on UAVs to Capture Paleoseismic Offsets

In this study, multi-view Photogrammetry was used to generate topographic data along the Altyn Taugh fault shown in Figure 2.7 below, which is located in the Northern Tibetan plateau, China. A DEM with 0.65m resolution and an orthophoto of 0.016m resolution was derived from high-resolution UAV images. These formed the basis from which piercing markers and offsets were reconstructed. A seismic offset is generally the land displacement caused by an earthquake (Kendra et al., 2014). Their spatial characteristics are usually assessed using 3D data, which provides the basis for mapping their complexities and offset distances.

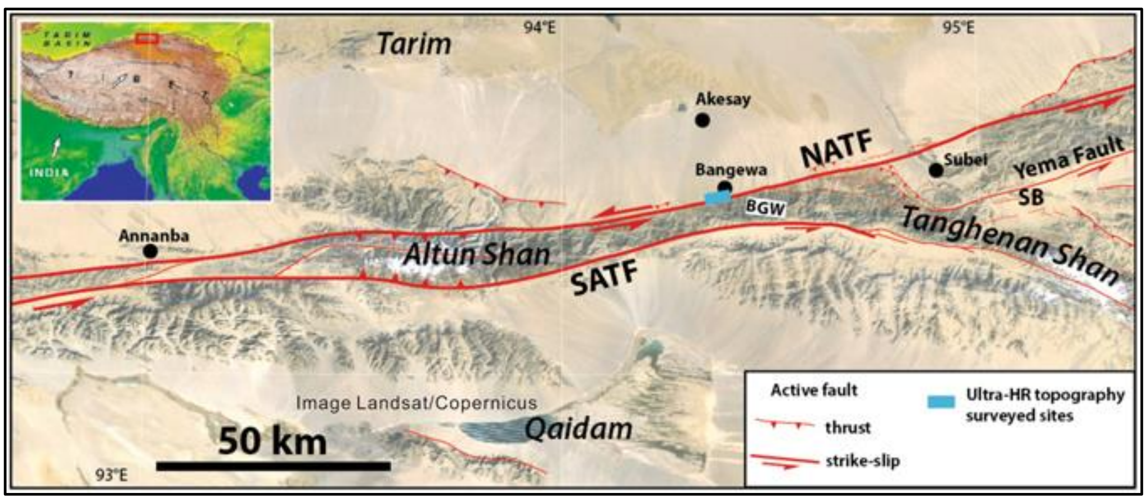

Figure 2. 7: Overview of the Northern section of the Altyn Taugh fault

Image source : https://www.ncbi.nlm.nih.gov/pmc/articles/PMC5557976/figure/Fig1/

Combined with a high-resolution satellite image, the cumulative measured offsets were 15±2m, 20±2m and 30±2m which was deemed to be as a result of multiple earthquakes. Typically, high-centimetre resolution satellite images like Quickbird and GeoEye are used together with airborne Lidar to map earthquakes over hundreds of kilometres. UAV Photogrammetry was therefore a low-cost alternative that took lesser time in data acquisition and processing.

The workflow involved taking low altitude UAV images to capture evidence of paleo-seismic deformations along the active fault. The cumulative faults identified were to be validated using SPOT satellite imagery.

Agisoft Photoscan was then used following a detailed procedure by Lucieer et al. (2014). The SfM approach was where the initial bundle adjustment formed a dense point cloud of 37million points. 12 GCPs spread across the study area were fixed using a handheld GPS for two rounds. Differential correction on the observations was later performed to 1m accuracy with RMSE values of 0.3m (X), 0.26m (Y) and 0.07m for the altitude (Z). The end result was a DEM of 0.065m vertical resolution and an orthophoto of 0.016m resolution which aided in the reconstruction of the seismic offsets as shown in Figure 2.8 and 2.9 below.

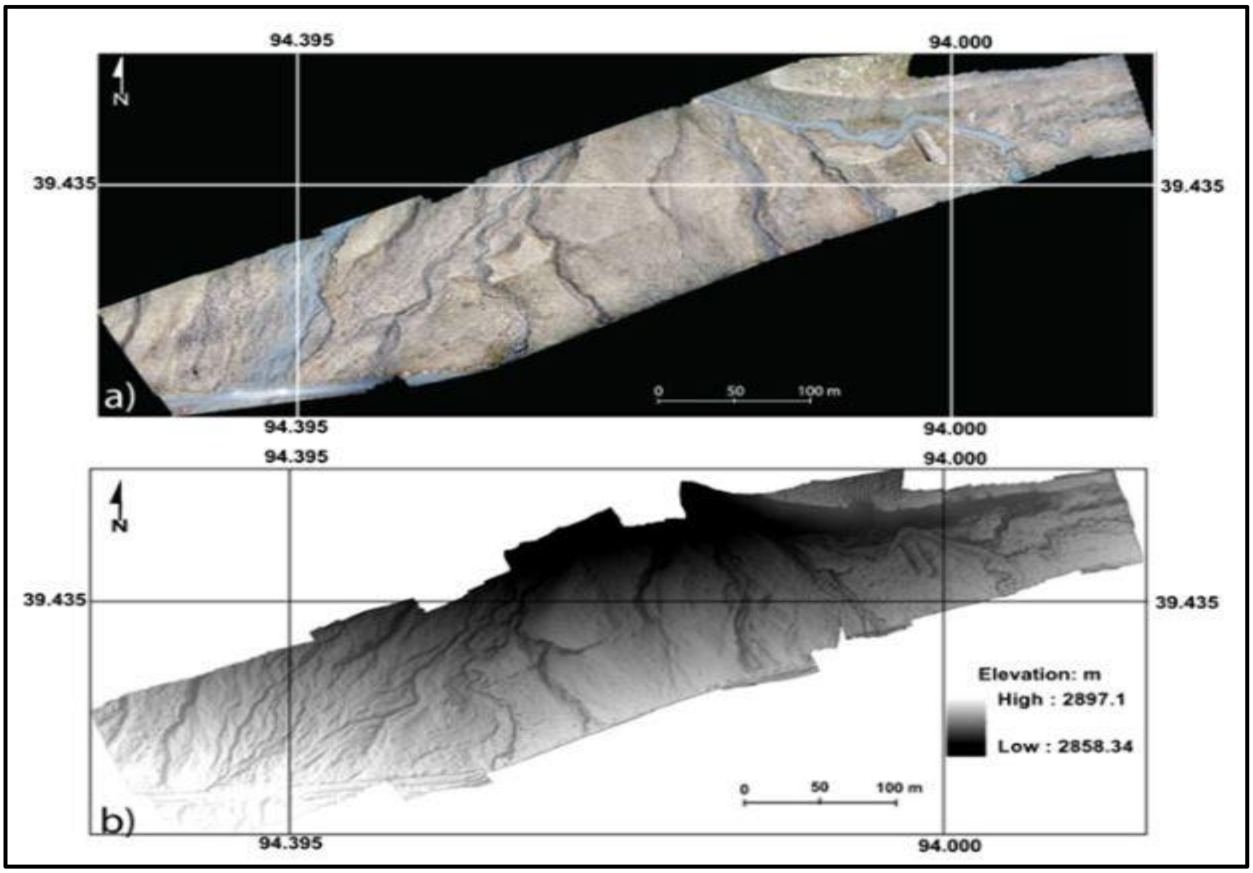

Figure 2. 8: The Orthoimage of the study area of 0.016 m resolution (a) and the high-resolution bare earth DEM of 0.065 m resolution, derived from UAV imagery (b)

Image source : *https://www.ncbi.nlm.nih.gov/pmc/articles/PMC5557976/figure/Fig6/*

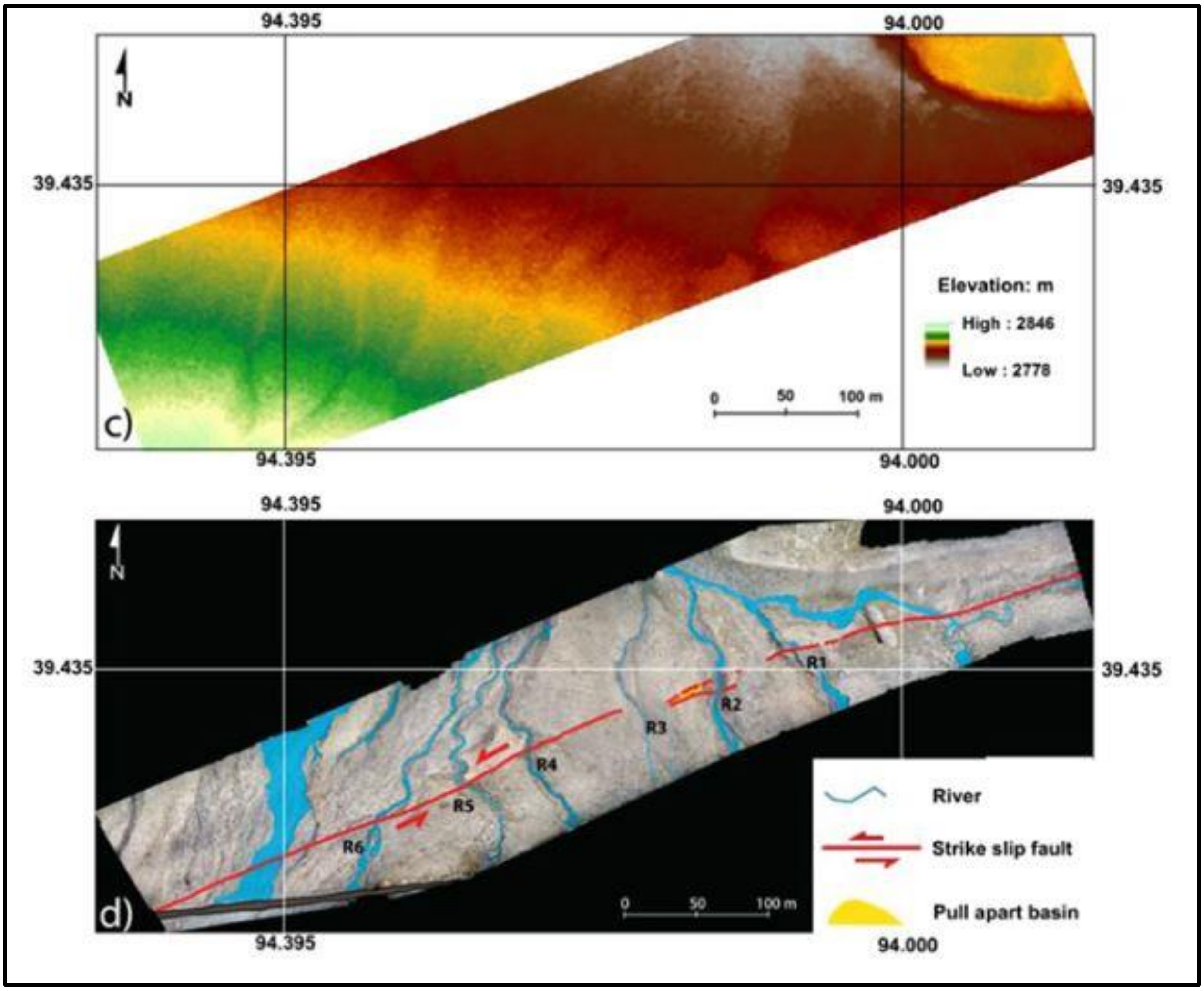

Figure 2. 9: A DEM of 0.5 m resolution calculated from a stereo pair of Pleiades satellite images (c) and the six streams (R1–R6) along the fault that were used to reconstruct the seismic offsets.

Image source : https://www.ncbi.nlm.nih.gov/pmc/articles/PMC5557976/figure/Fig6/

The faults were located accurately, and offsets reconstructed by assessing the topography along the 6 streams as shown in Fig. 2.9.

In this study, it was ascertained as well that UAV imagery was best suited for such a project owing to its cost-effectiveness and ability to generate high resolution 3D datasets in a very short amount of time.

2.5.3 Estimating Tree Heights with Images from UAVs

In Forestry, tree heights and crowns are usually estimated with different Remote Sensing technology such as airborne or spaceborne Lidar systems, which are often expensive to commission. In this research example, UAV Photogrammetry was proven to be very convenient especially in monitoring tree species and their characteristics. UAV imagery was used to obtain individual tree heights in a man-made forest called the Urban Forest of Eskisehir City, Turkey shown in Figure 2.10 below.

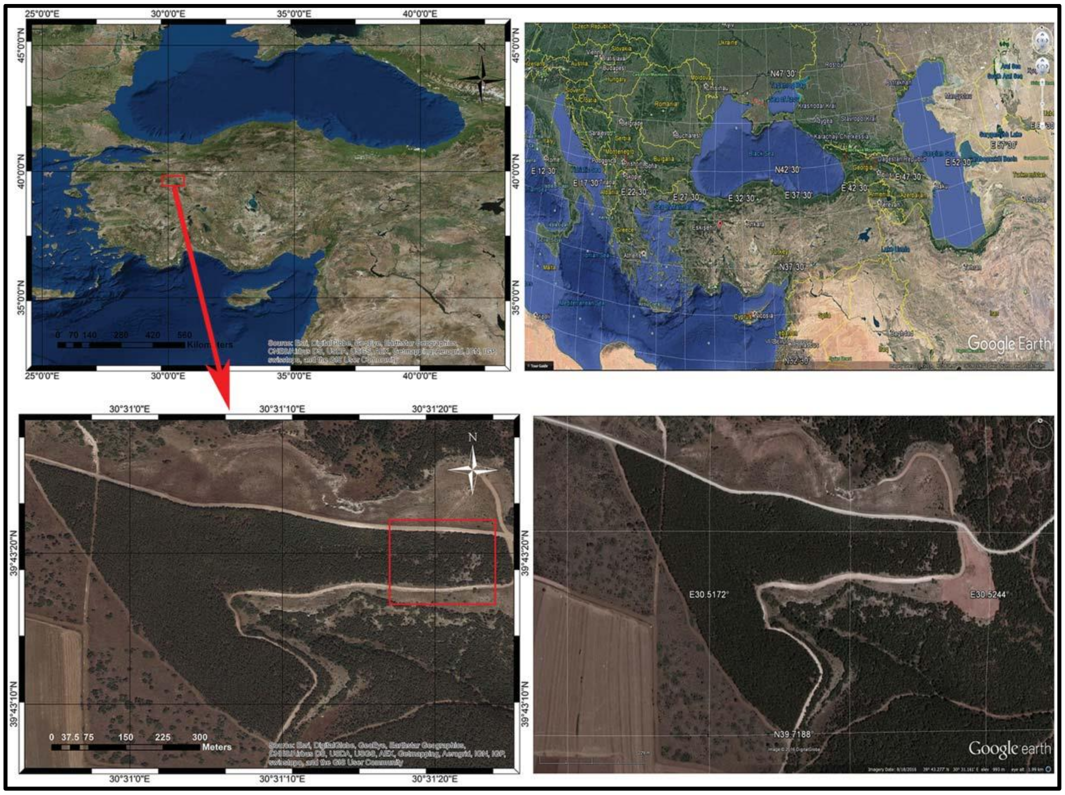

Figure 2. 10: The Urban Forest of Eskisehir City, Turkey

Image source : *https://www.tandfonline.com/doi/full/10.1080/19475705.2017.1300608#*

The workflow involved flight planning, image acquisition and obtaining GCPs. Ground measurements of the tree heights were also taken that would serve as a validation reference. The figure below summarizes the study workflow that was implemented:

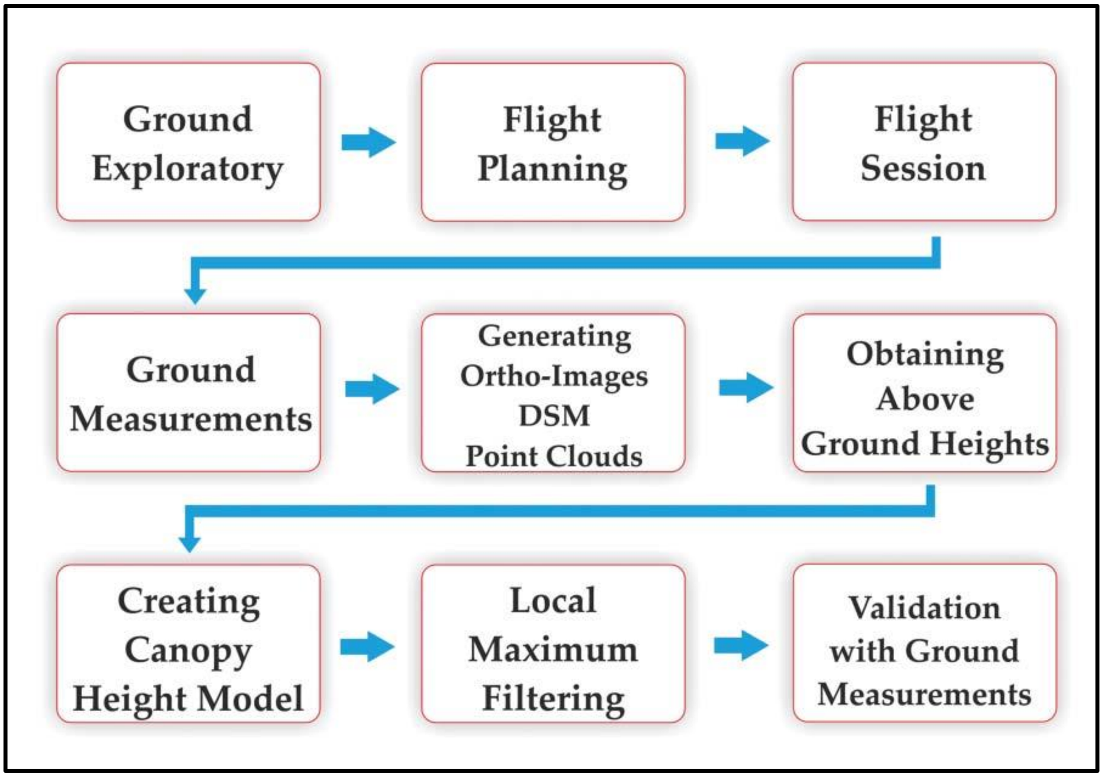

Figure 2. 11: The study workflow

Generating the ortho-images and point cloud was a semi-automatic process with the only manual part being the marking of GCPs. This was done using Pix4D software as shown in Figure 2.12 below:

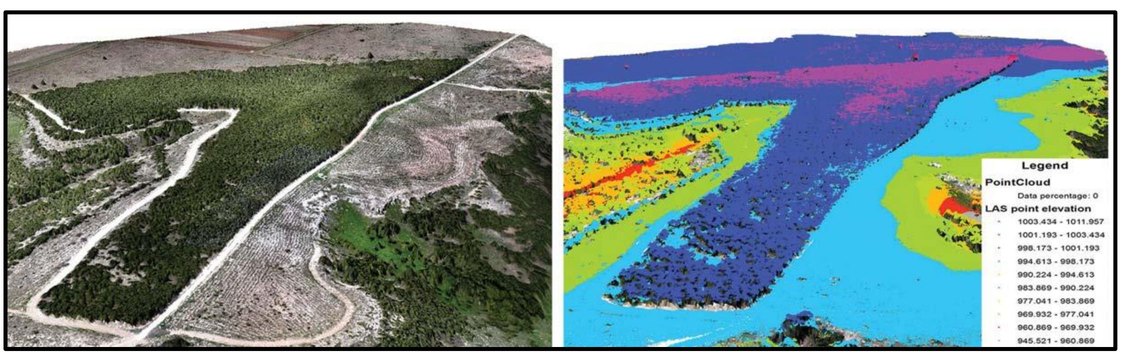

Figure 2. 12: The DSM (left) and the point cloud (right) of the study area.

Image source : https://www.tandfonline.com/doi/full/10.1080/19475705.2017.1300608

The GCPs measured had a RMSE 0.004m. 133 images were afterwards calibrated giving rise to 1.7million key points for bundle adjustment. The resulting point cloud was then classified into two; ground and non-ground points to facilitate the reconstruction and texturing of a digital terrain (DTM) and surface (DSM) model. The canopy height model was then generated by subtracting the DSM from the DTM. The ground-based measurements made gave a 94% correlation and a RMSE of 28cm. Using a software known as FUSION LVD, the researchers were able to apply a local maximum filter to further distinguish between the tree species on the DSM.

Finally, 53 trees were measured using a laser distance meter and compared to the estimated tree heights for validation and the results plotted as shown in Fig. 2.13 below. The linear regression parameters and correlation coefficients were also shown in the plot.

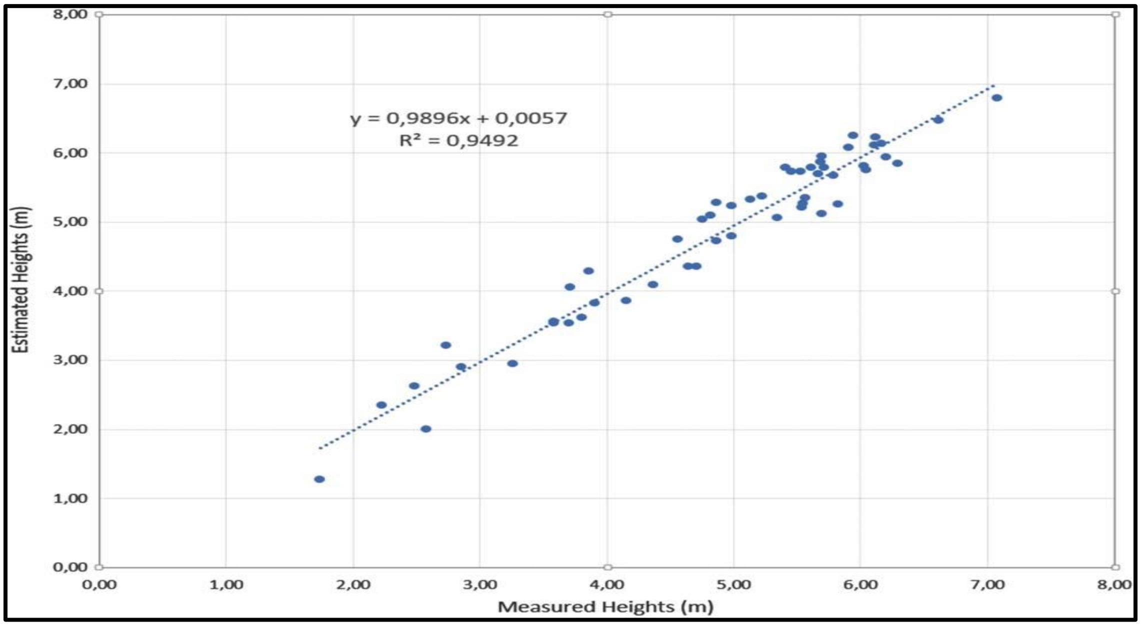

Figure 2. 13: Validation results for 53 measured tree heights against the estimated heights.

Image source : https://www.tandfonline.com/doi/full/10.1080/19475705.2017.1300608

As can be seen from the results above, measurements compared to the algorithm-derived datasets were pretty much acceptable. This proved that 3D data obtained from UAV imagery is very much reliable and the technology effective in keeping forest inventories, among many other applications.

CHAPTER 3: MATERIALS AND METHODS

3.1 Study Area

The Study area was confined to Nairobi City County, specifically along Thika Superhighway. It spans about half a kilometre from Muthaiga interchange to Muthaiga Primary School. There is already adequate data for the specific road section and surrounding scenery to make an informed generalization of the study topic for the entire County. Figure 3.1 below shows the study area.

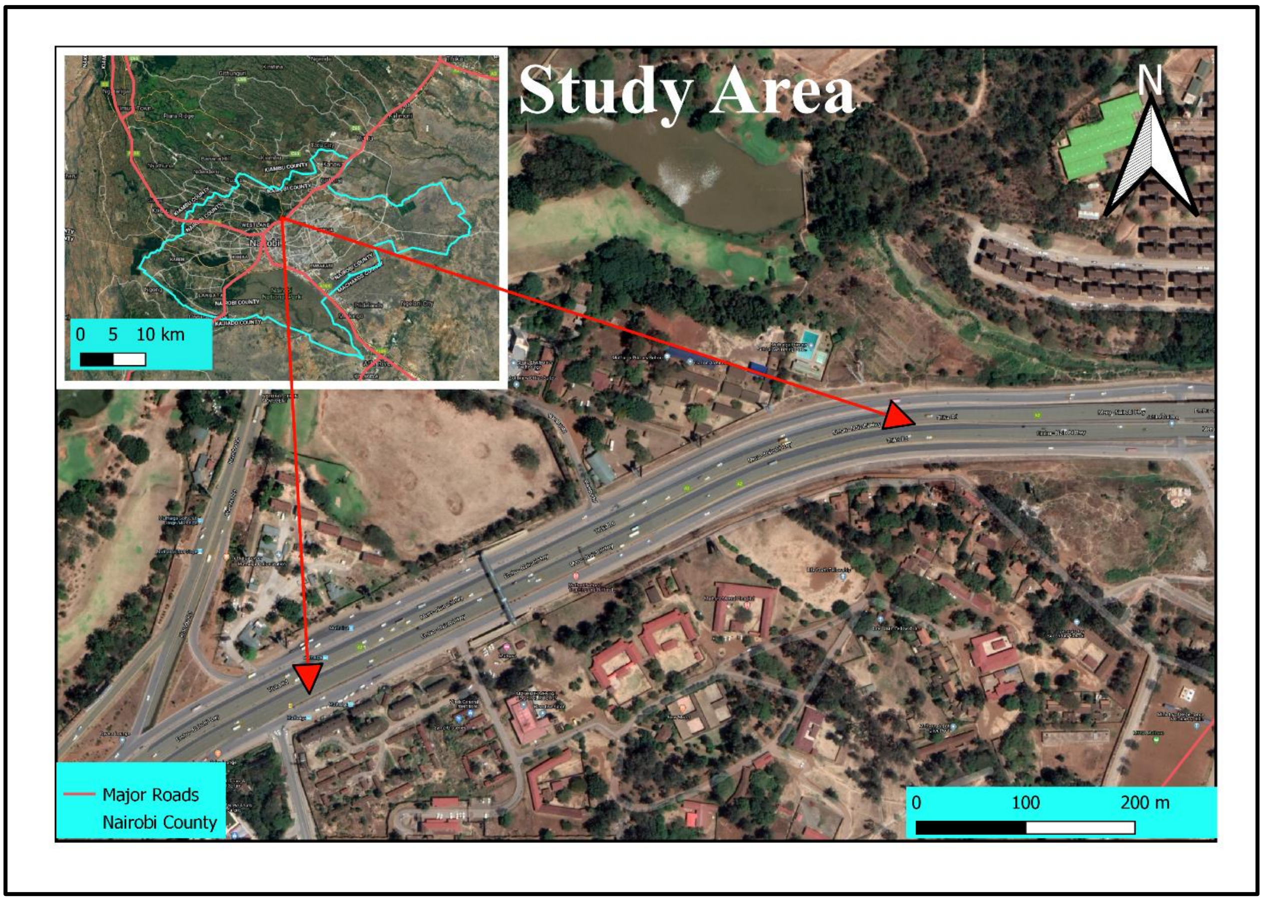

Figure 3. 1: Area of Study

3.2 Data and Data Sources

The main data (UAV imagery) that had been acquired for a different purpose was obtained from Mr. Fredrick Arthur Onyango (See Acknowledgements). The actual billboard measurements were acquired from field observations. Terrestrial high-resolution images of the study area were also acquired using a digital camera for comparison and contextual information.

3.3 Materials and Equipment

Table 3. 1: Summary of equipment and their specifications

Equipment	Specifications
Personal Computer	Dell inspiron I5 7000 Gaming laptop, octa-core 2.8Ghz processor, 16 GB RAM, dedicated 4GB Nvidia Geforce GTX graphics card
Leica Robotic Total Station	Series TCRA 1203+
Hand-held GPS receiver	Garmin Etrex 30
Samsung digital camera	ES80, 13.1MP, 5x optical zoom

Table 3. 2: Summary of software and their respective versions

Software	Version
Windows 10	Professional (64-bit)
Agisoft Metashape	Version 1.9 (Proprietary software solution)
Microsoft Office	2016

3.4 Workflow and Methodology

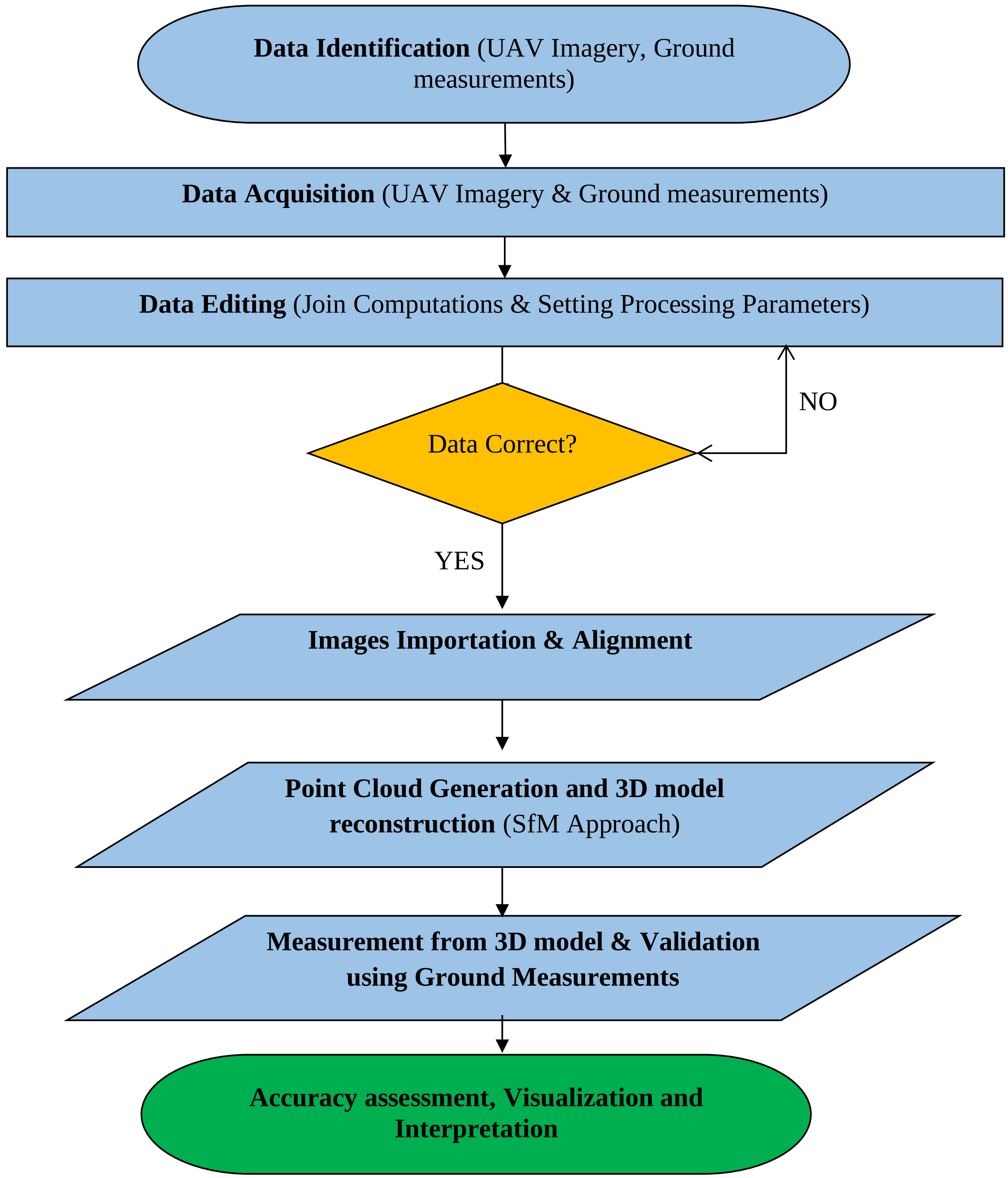

Figure 3. 2: Flow chart showing an overview of the methodology

3.4.1 Field Data Collection

The actual dimensions of the billboards within the study area were taken using a robotic total station (Leica TCRA 1203+). The following procedures were used to collect the data:

i) A suitable observation station was chosen, and standard survey procedures used to mount and level the equipment on the tripod.

ii) Since the dimensions of the billboards were to be taken without contact, the measuring method in the total station was changed from prism to “reflectorless”.

iii) A hand-held GPS receiver was used to roughly estimate the direction of the azimuth using its compass, then the total station was rotated to point towards North and the horizontal circle set at 00° 00' 00" for orientation. The vertical circle of the equipment is normally calibrated hence there was no need to pre-set its parameters.

iv) The GPS was also used to get a lock on the position of the total station, with an accuracy of 2 meters. The coordinates were fed into the total station as our known point and basically orients the equipment on the horizontal plane, ready to point to the next target. The instrument height was also fed in as 1.615 meters. This would aid in automatic computation of target heights.

v) After the instrument was oriented, it was rotated in a clockwise direction to point to the first target, which was the bottom left corner of the first billboard, to get the bearing and distance. Figure 3.3 Below shows the convention and order in which the three corners of the billboards were named and measured. For the first billboard, the corners were notated in a clockwise direction from the bottom left corner as P11, P12 and P13. For the second billboard, P21, P22 and P23 and finally P31, P32, and P33 for the third billboard. The table below summarizes the measurements taken from three billboards:

Table 3. 3: Summary of measurements taken by the robotic total station

Billboard 1	**Horizontal Angle**	**Vertical Angle**	**Horizontal Distance**	**Height of Target (HOT)**
P11	155° 36' 17"	81° 57' 48"	42.895m	6.031m
P12	155° 34' 44"	68° 08' 05"	42.883m	18.084m
P13	169° 06' 59"	66° 05' 20"	41.052m	18.084m
Billboard 2				
P21	149° 25' 41"	85° 51' 17"	114.248m	8.281m
P22	149° 24' 58"	79° 56' 16"	114.607m	20.338
P23	154° 10' 22"	79° 33' 47"	110.958m	20.439m
Billboard 3				
P31	111° 57' 03"	87° 27' 54"	164.733m	7.295m
P32	111° 51' 02"	83° 49' 16"	165.254m	17.893m
P33	116° 48' 27"	83° 28' 42"	159.756m	18.265m

Figure 3. 3: Billboard measurements being taken using a total station

3.4.2 Join Computations

Join computations refer to calculations done to derive the distance and bearing from one point of known coordinates to another point of known coordinates. Since the coordinates of the station occupied had already been established, the main task was to deduce the coordinates of the target points, which were the three corners of the billboards. These coordinates would then yield the joins (distance and bearing of one billboard corner to another), which in essence would be the length and width of the billboards. There was no need for measuring the fourth corner since the dimensions can be deduced from the three corners. A fourth point would have been simply redundant.

In order to obtain coordinates of unknown points from known points using distances and bearings, rectangular coordinates had to be computed. This was done automatically using a scientific calculator but the fundamental principles involve computing the displacements in the cartesian plane (ΔX and ΔY) then adding the displacements to the known coordinates or origin (O) in order to obtain coordinates (X2,Y2) of the unknown point P, as illustrated in Figure 3.4 below.

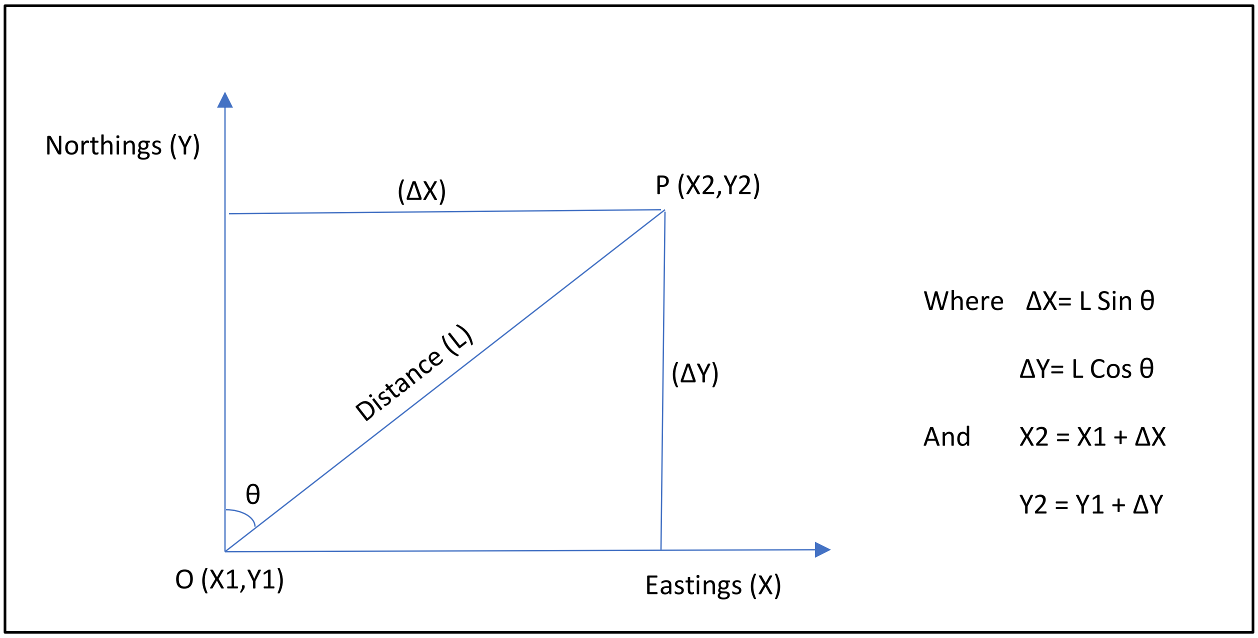

Figure 3. 4: Computing Rectangular coordinates

Using a scientific calculator, the "Rec" function for computing rectangular coordinates was used whereby the distance then bearing was input, separated by a comma. The first result is usually ΔY. To obtain ΔX, the combination RCL (Recall) + F was used.

After obtaining the coordinates of the three corner points of the billboard, the final step is to compute the join (distance and bearing) from one cornet to another. It is worth noting that the joins across the horizontal plane (corner points P12 to P13, P22 to P23 and P32 to P33) were the most crucial given that they deduced the horizontal length the billboards. The vertical length or heights were simply obtained by subtracting the heights of targets (P12 from P11, P22 from P21 and P32 from P31) which were automatically recorded by the total station. From Figure 3.4, this would basically involve deducing the distance L and bearing θ. Since the coordinates of the two points are now known, ΔX and ΔY can be computed, from which L and θ can be deduced by making them the subject in equation.

Using a scientific calculator, the "Pol" function was used whereby ΔY and ΔX were input in that order, separated by a comma. The first result is usually the distance. To obtain the bearing, the combination RCL +F was used. It's worth noting that if the result of the bearing is a negative value, 360° is added to make it a true bearing (Horizontal angle measured clockwise from true North). All these computations were done on standard Survey computation sheets (Refer to Appendices A, B and C).

3.4.3 Setting Image Processing Parameters and 3D model Reconstruction

Before Image processing, certain parameters have to be set that would determine the quality of the 3D render and how long the process takes. The processing settings are usually adjusted to match the hardware capabilities of the computer being used. The computer used for this study had good hardware specifications (See Table 3.1) that were able to meet the computing demands of the software. For this reason, most of the settings were left as default while a few were tweaked to optimize the results at various stages.

Agisoft Metashape was launched and the reference system first set to UTM in order to be able to make measurements in the metric system. All other values in the reference system were left at default as shown on Figure 3.5 below.

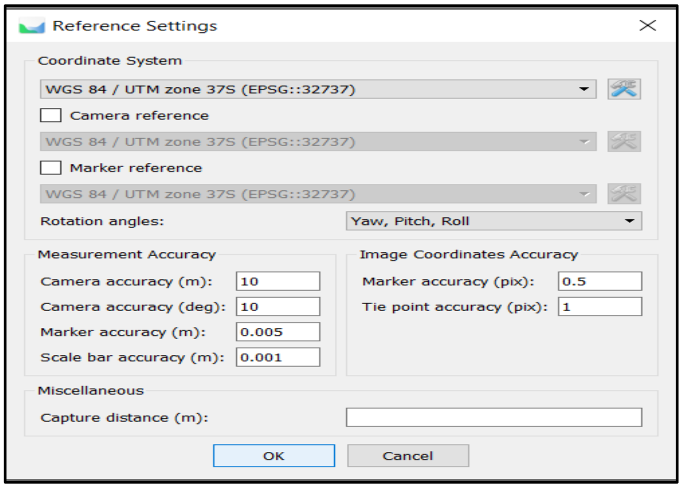

Figure 3. 5: Reference settings

Before importing any images, most of the workflow menu items were greyed out. This was intended for sequential execution of the processes required for the final output.

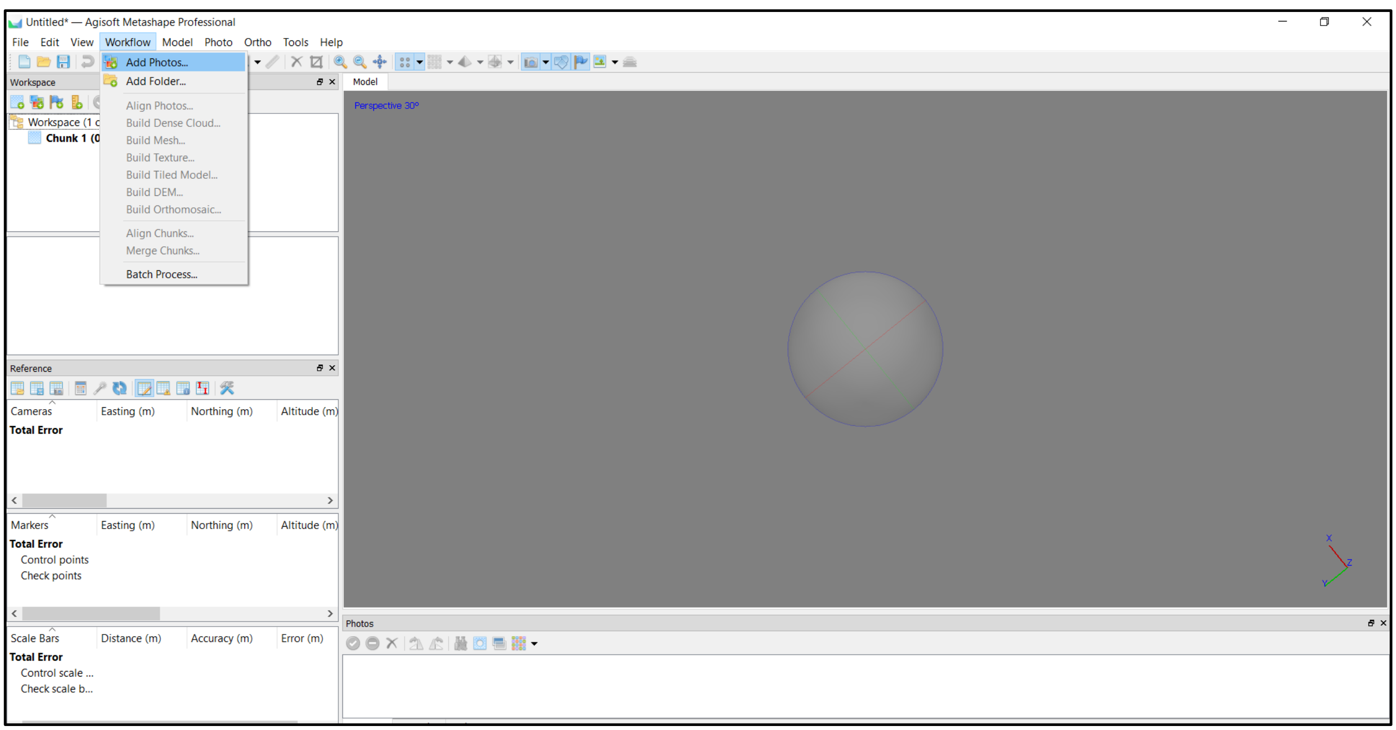

Figure 3. 6: Agisoft Metashape Interface showing the Workflow menu.

From Figure 3.6 above, the sequential order of operations can be seen. After adding photos, they were aligned, a dense cloud built, followed by a mesh, the model textured then finally exported. The other menu options like creating a DEM or Orthophotos were not required for this study.

The UAV images were then imported into Agisoft Metashape. The coordinates of the image spaces were automatically populated and a grid showing the location of each individual photo in space displayed as shown in figure 3.7 below.

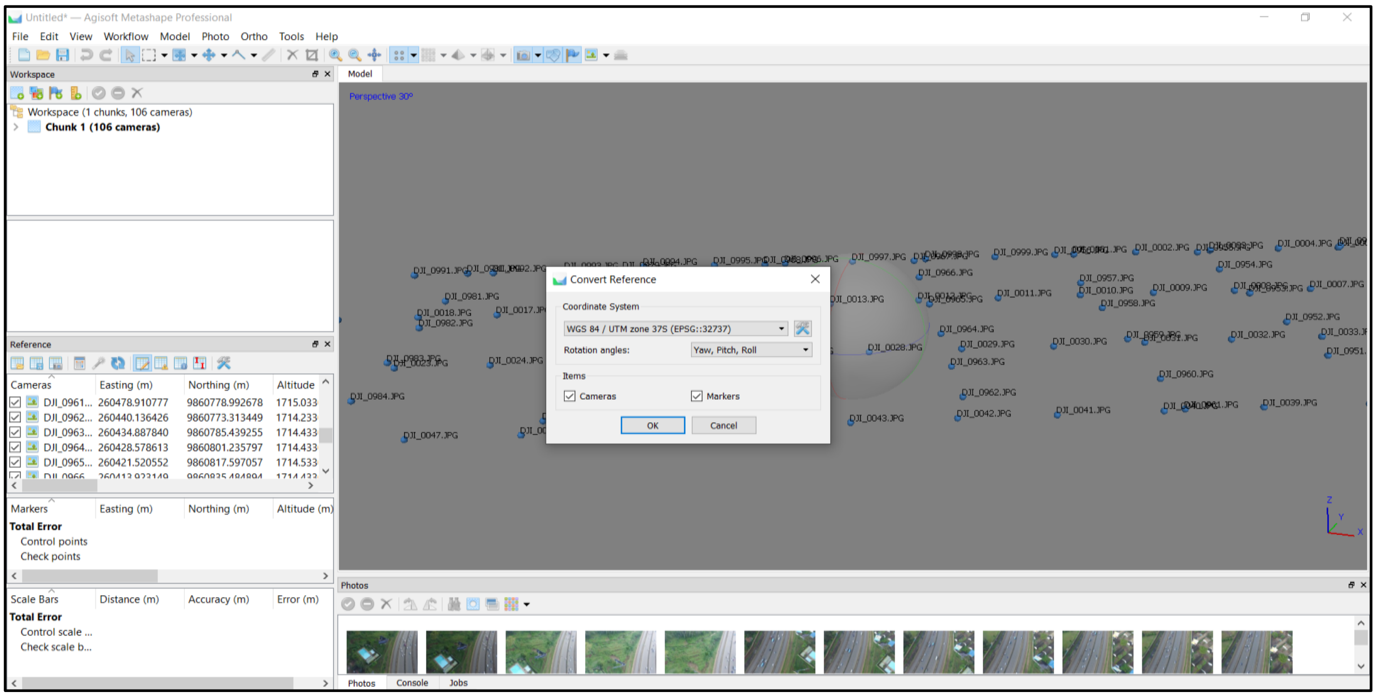

Figure 3. 7: Imported images showing a grid of computed locations for each photograph

The next step was aligning the photos. As shown in Figure 3.8 below, both generic and reference preselection options were checked. Generic preselection scans all the photos for tie points hence significantly increases the processing time but reference preselection localizes this search and restricts it to nearby or surrounding photos in the alignment sequence. Since the photos acquired did not have ground control points, it was prudent to check both options to maximize chances of automatic tie-point identification.

In advanced options, the key point limit was set to 240,000 for best results and zero on the tie point limit. Setting zero basically renders the number of tie points limitless.

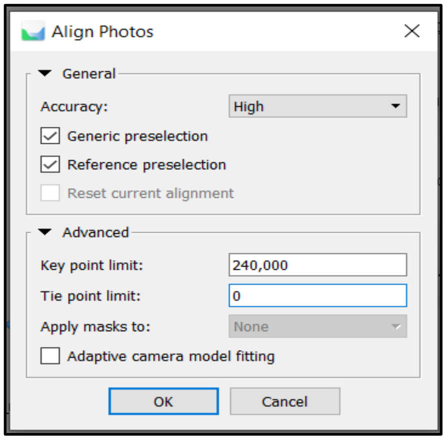

Figure 3. 8: Setting general and advanced preselection parameters before alignment

While processing, the software displayed the number of points generated from each photo and adjustment parameters among many others, as shown in Figure 3.9 below.

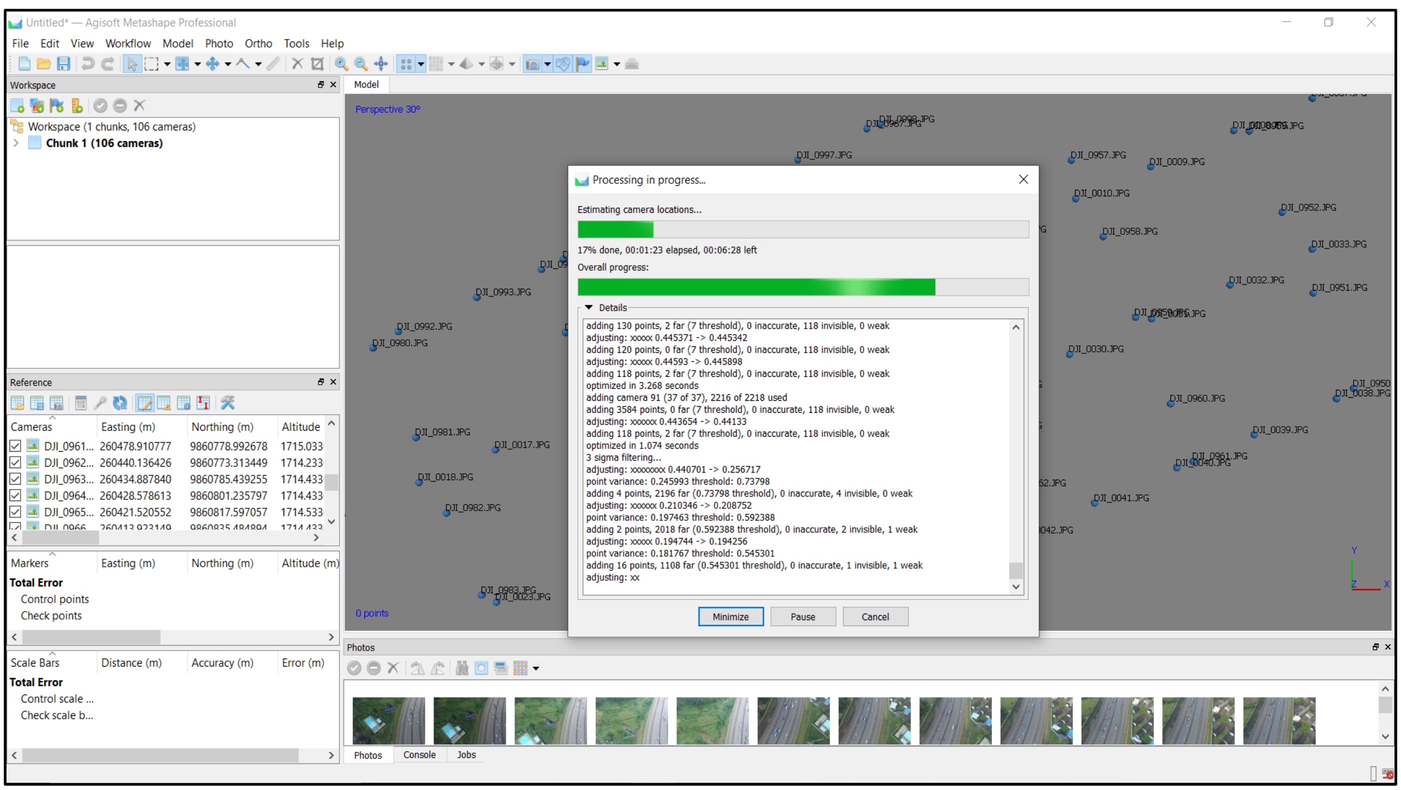

Figure 3. 9: Image alignment progress bar and adjustment parameters

Once alignment was done, a sparse point cloud was generated as seen in Figure 3.10 below with camera positions visible. This could be rotated to get a better view of the scenery. In total, 304,795 points sparse points were generated, and 106 images aligned.

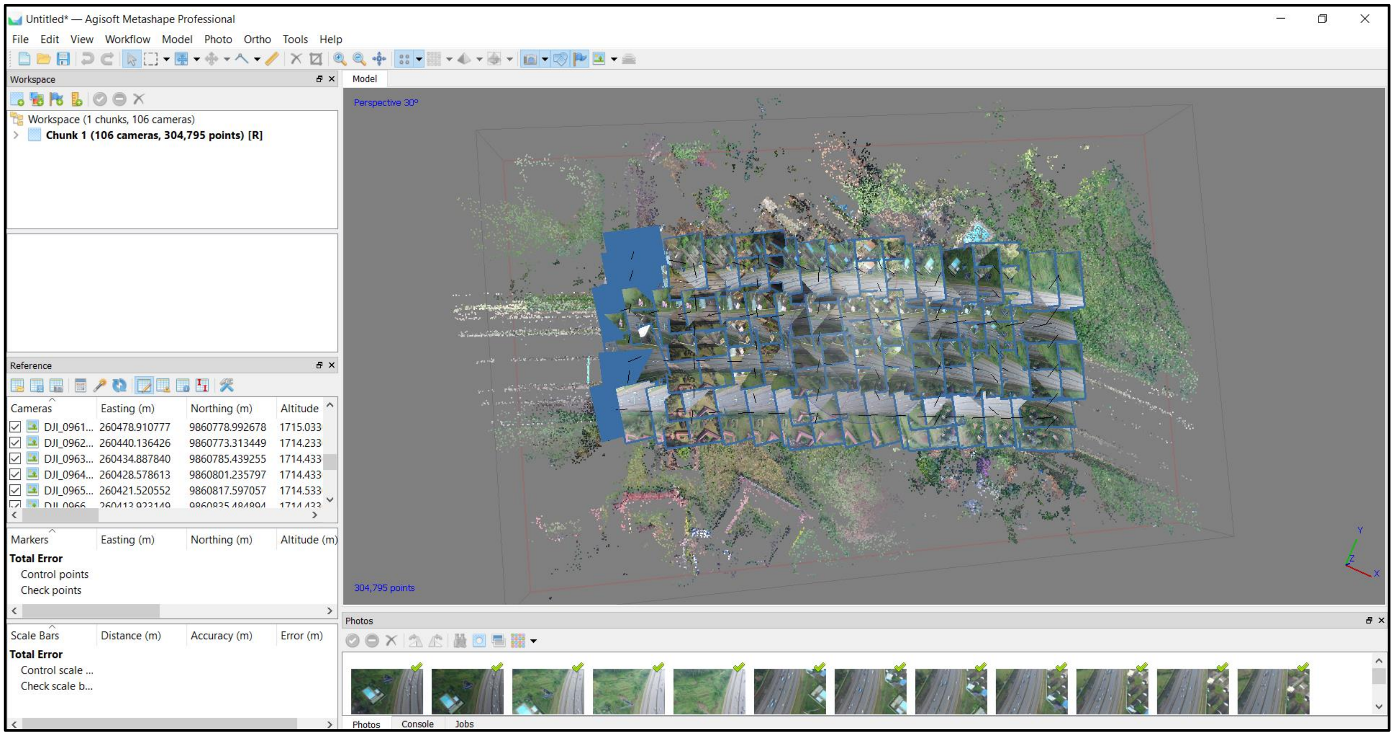

Figure 3. 10: Aligned images with visible camera positions and a sparse point cloud

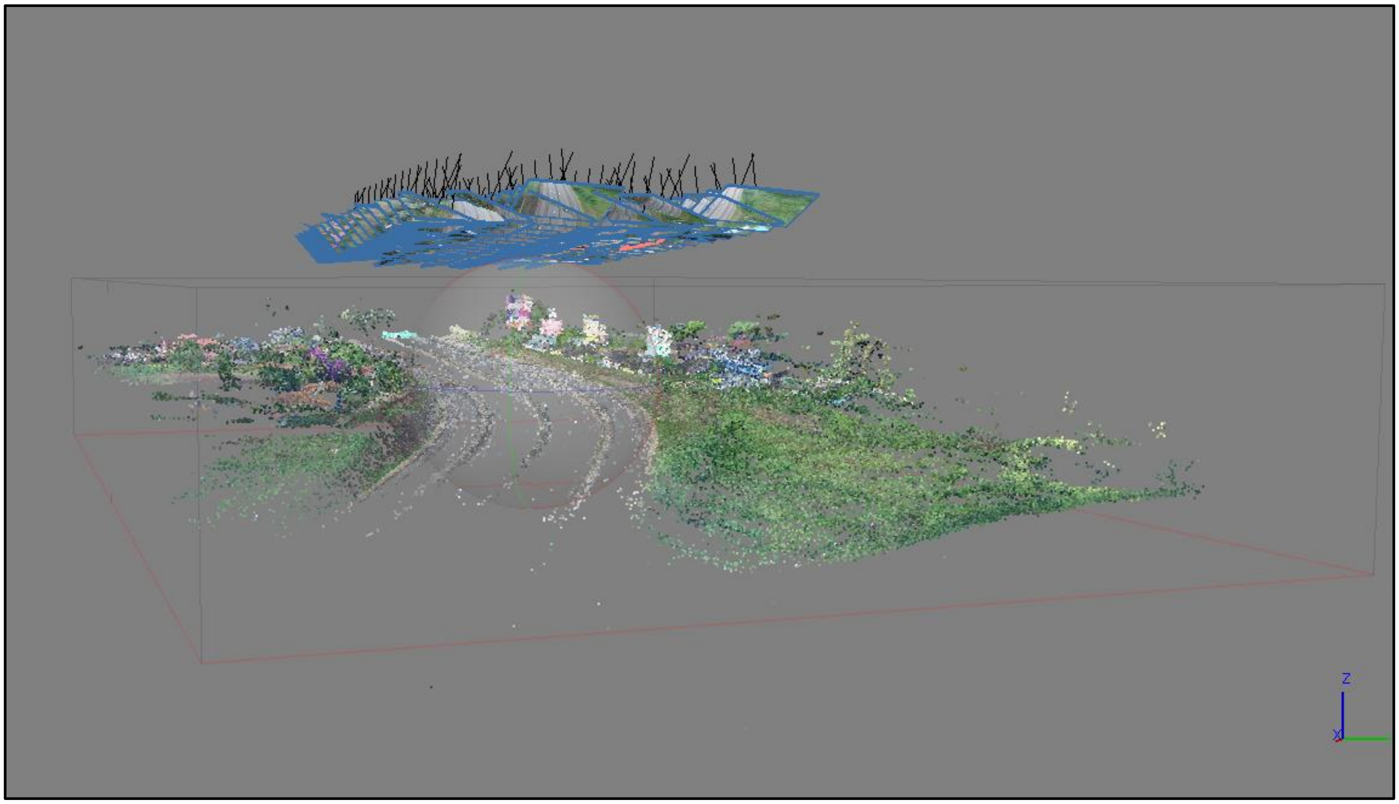

Figure 3. 11: Bounding box showing the extent of data viable for further processing

As seen from Figure 3.11 above, the bounding box in black and red defined the extents of the data acquired and viable for further processing. Anything outside of this box was disregarded by the software. If the images had Ground Control Points, they would have been imported at this point and the tie point positions updated. In this project, the structural accuracy of the model was of more importance than its spatial or positional accuracy hence the GCPs were not really imperative. The drone that was used to capture the images (DJI Phantom 3 Professional) had an inbuilt GPS/GLONASS that captured positional information. The photos were hence already georeferenced albeit with a spatial accuracy of 10 meters.

The next step involved generating the dense point cloud. However, the camera positions had to be optimized before generating the dense point cloud by clicking on the "Reference" tab then "Optimize Cameras" option. Upon clicking the "Build Dense Cloud" option from the workflow menu, a dialogue box appeared that prompted further parameter adjustments before processing. The quality option was set to "High" and In-depth filtering set to "Aggressive" for best results. This was the most time consuming and RAM intensive step. It could take a few minutes or last for even hours depending on the computer specifications. The computer used in this project took 38 minutes and 25 seconds to generate a dense point cloud as seen on Figure 3.12 below.

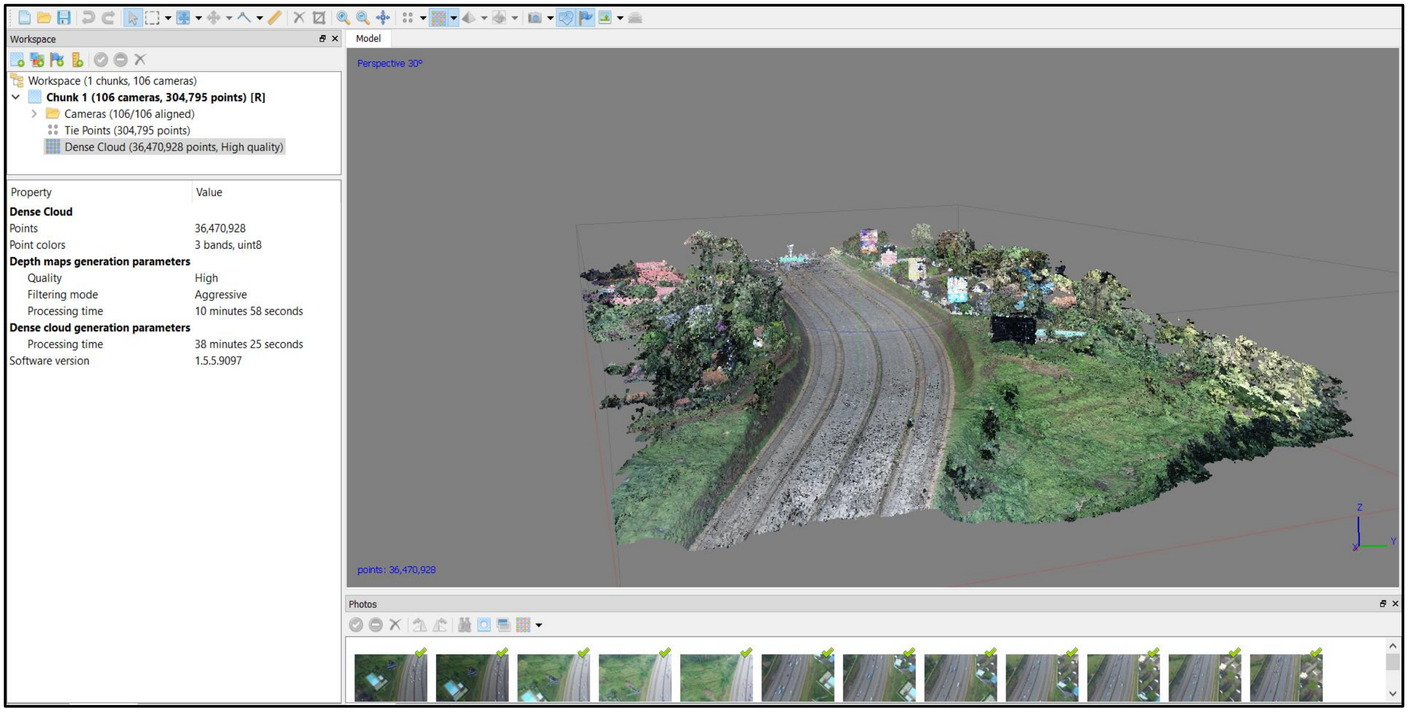

Figure 3. 12: Dense point cloud showing depth map and cloud generation parameters

The dense cloud consisted of 36,470,928 points. The physical features of the area of study could then be distinguished clearly and the main subject of interest, the billboards, were made distinct and visible. It’s worth noting that the software has superior algorithms for automatic detection and masking of moving objects. For this reason, the resulting point cloud generated had no cars on the roads, which gives a smoother render of the scenery.

The final steps involved building a mesh to enjoin the dense point cloud then finally texturing the model to render a photorealistic model of the study area. Both steps were executed sequentially in the workflow menu using default parameters to yield a 3-D georeferenced scenery from which distinct features can be identified as shown in figure 3.13 below.

Figure 3. 13: The textured model with distinct physical features and billboards

CHAPTER 4: RESULTS AND DISCUSSION

4.1 Measurements from the 3-D Model

The generation of a dense point cloud, building the mesh and subsequent texturing resulted into a georeferenced, 3-Dimensional model of the study area. This meant that screen measurements and coordinates would represent the actual measurements or coordinates on the ground with minimal errors.

From the ground measurements, the dimensions of three billboards were acquired from the most strategic point within the study area. Two billboards were observed on the same side as the observation station, and one across the road. However, upon generating the 3-D model, it was noted that the billboard across the road was not captured. Upon inspecting the UAV images, it was apparent that the billboard was not in existence as at the time of image capture. This meant that only two billboards out of the three could be validated, having taken their ground measurements, which was still good enough for purposes of comparison and validation.

From the screen measurements, the first billboard had a length (P12-P13) of 10.0m and a height (P11-P12) of 12.1m as shown in Figure 4.1 below.

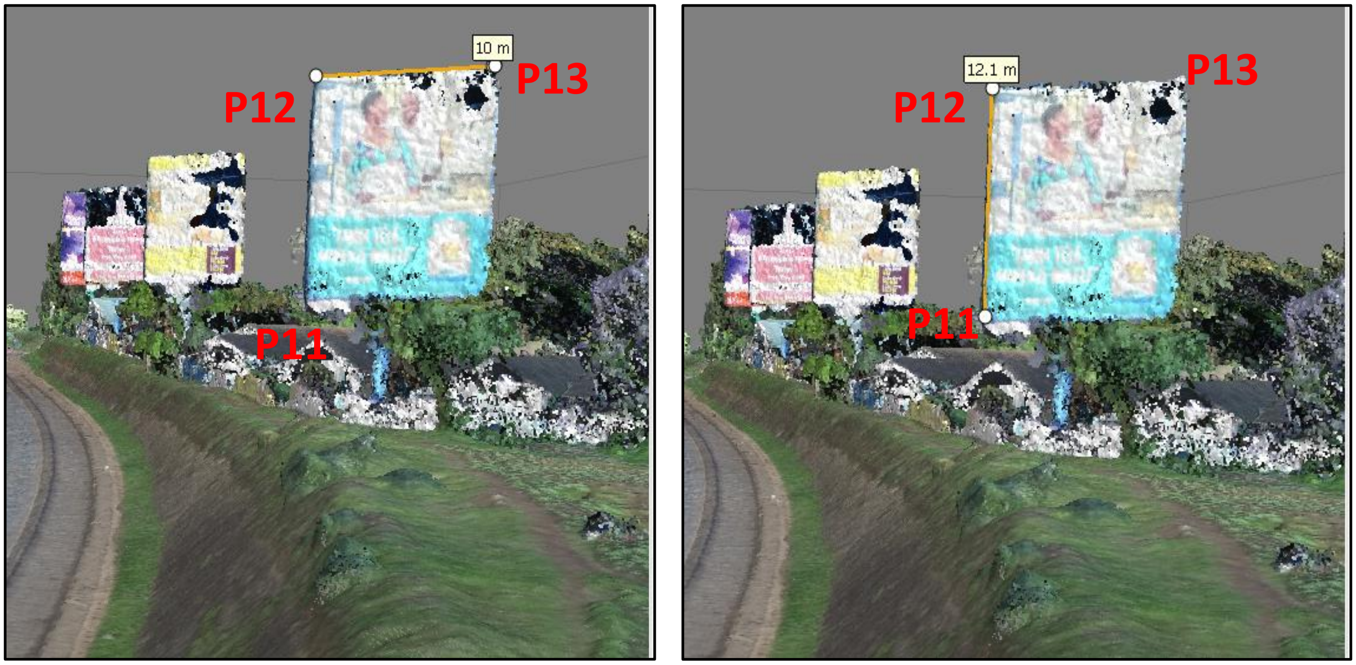

Figure 4. 1: Screen measurements of the first billboard showing its span and height

The second billboard on the other hand had a length (P22-P23) of 9.99m and a height (P21-P22) of 12.1m as shown in Figure 4.2 below.

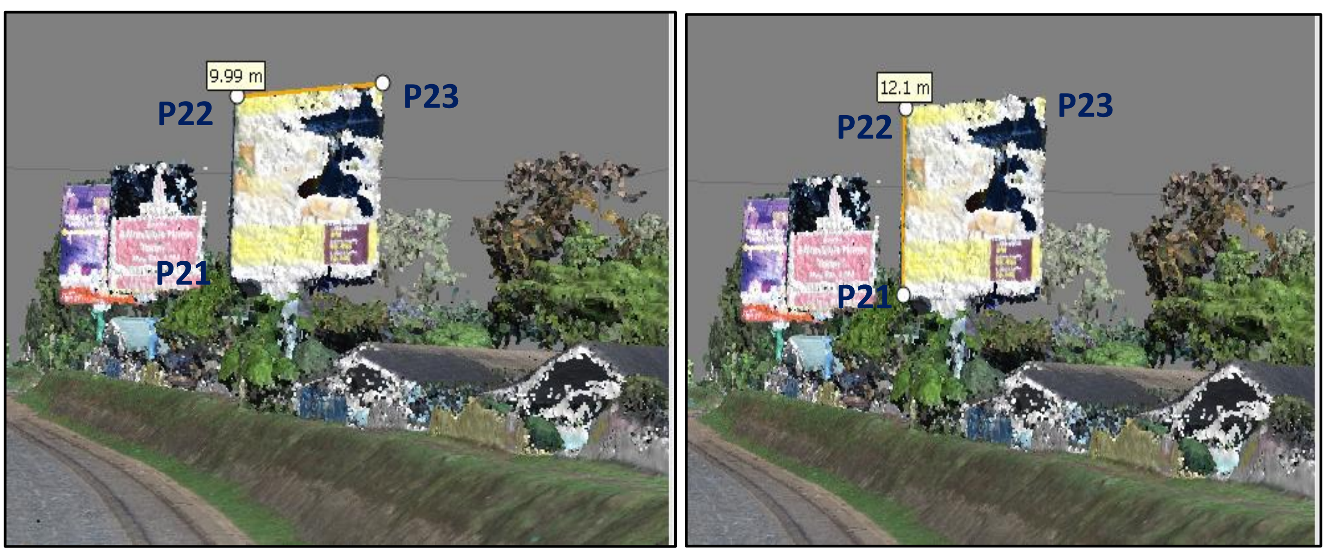

Figure 4. 2: Screen measurements showing the span and height of the second billboard

4.2 Validation of Dimensions using Ground Measurements

Having measured the dimensions of the billboards using the model, the same measurements were compared to the ground measurements previously taken using a total station as seen in appendices A and B. Table 4.1 below summarizes the dimensions of the billboards measured through the two methods.

Table 4. 1: A summary of the measurements taken using the model and the total station.

Billboard1	Model Measurement	Precision	Ground Measurement	Precision	Difference (meters)
Length (m)	10.00	± 0.1	10.059	± 0.01	0.059
Width/Height (m)	12.10	± 0.1	12.053	± 0.01	0.047
Billboard2					
Length (m)	9.99	± 0.1	10.045	± 0.01	0.055
Width/Height (m)	12.10	± 0.1	12.057	± 0.01	0.043

4.3 Discussion of Results

As seen from the measurements in Table 4.1, there is no significant difference in measurements given that the differences in dimensions were no more than 0.059meters (about 6 centimetres). For this study, this was a very good result given that billboard dimensions vary in terms of meters. This meant that to deduce the actual dimensions of a billboard from the model, we could simply round the measurement off to one decimal of a meter. Therefore, for a measurement such as 9.99 meters, the true length would be 10 meters, and 12.1 meters would be simply 12 meters et cetera.

To further solidify the hypothesis that there could be no statistically significant difference between the two methods of measurements, statistical tests like the Student's t-test or Regression analysis could have been performed. With a sample size of only four pairs of measurements, the results would have had a low statistical power. The sample size should be large enough to estimate the variances, meaning several billboards would have to be measured. However, this would have been transcending the project’s scope, whose main objective was to simply show that model measurements can be reliable in deducing billboard dimensions, and not to statistically make a comparison of their accuracy with regards to the total station measurements.

The specific objectives of the study were met where a 3-D render of the study area was successfully modelled, and its geometric accuracy assessed by inspection. The physical feature rendered were representative of the actual features on the ground and the main subject of the study, the billboards, could be clearly distinguished and measured. The model measurements were also validated by comparing them to the ground measurements where the differences in measurements were ranging between 0.043 and 0.059 meters.

Compared to other methods of conducting such a study, using a UAV may prove to be most efficient since it does not even require highly experienced personnel to operate. Operation manuals and tutorials are readily available online so interested individuals and corporates can easily build capacity to conduct such studies. The quality of results may only be affected by the type of UAV used and the method employed to capture actual ground measurements. Typically, professional drones should be used that have in-built GNSS receivers and a high-quality RGB or multi-spectral camera. However, for small study areas, consumer-grade drones can also be used albeit in conjunction with powerful Photogrammetric Software such as Agisoft Metashape that employ SfM algorithms to reconstruct the scenery.

CHAPTER 5: CONCLUSIONS AND RECOMMENDATIONS

5.1 Conclusions

Having successfully acquired accurate measurements and comparison with model measurements found to be acceptable, it can be concluded that using UAV imagery offers a cheaper and faster alternative to ascertaining billboard measurements for purposes of revenue projections, inventory keeping and monitoring. Other methods like spaceborne LIDAR, UAV-LIDAR and even traditional Photogrammetric techniques can also work, but they're expensive, time consuming and may suffer some setbacks like cloud cover.

The Nairobi City County Government and other county governments for that matter, may find this study invaluable given the present state of outdoor advertising. The project can be scaled up to cover an entire county with the following potential benefits:

- **Asset Monitoring** – The County Government would be able to monitor the number of billboards occupied at any given time, their location and condition. This will help crack down on illegally erected billboards thereby ensuring compliance to set regulations and ensuring sustainable outdoor advertising.
- **Improved Revenue Collection** – Knowing the number of billboards and their occupancy state, the County Government can easily make an inventory of the billboards and make follow-ups on payments due given that some advertisers evade paying advertisement fees through corrupt means.
- **Accurate Revenue Projections** – Having the exact number of billboards within a county and their sizes, accurate revenue projections can be made which in turn inform achievable revenue targets set in tandem with the Annual Development Plan.
- **Smart Advertising** – Given that the location of the billboards can be known, this information can be integrated with other datasets like urban demographics to deduce optimal advertising locations and even charge premium rates for such locations where augmented reality and smart features that interact with the target audience can be incorporated to make the advertisements more compelling.

5.2 Recommendations

The overall and specific objectives of this studies were met despite several challenges from which the following recommendations can be assimilated:

i. Now that there exists a legal framework to fly UAVs in Kenya, more UAV images should be employed in similar studies to improve the texture of the model and make features more resolute.

ii. Recent photos of the scenery to be rendered should be taken to avoid discrepancies or missing data in the model generated. In this study, one billboard that was present and measured on site was missing in the model due to the fact that it had not been erected at the time of image capture.

iii. In order to make the model spatially accurate to sub-meter levels, more GCPs should be incorporated before image capture. This should be done during flight planning where bright objects whose precise coordinates are known would be placed strategically along flight paths to be later used during image matching using tie points, a procedure that the software carries out automatically after importing the GCPs.

iv. Future studies may also consider building a georeferenced 3-D database from which the billboards can be visualized and their metadata stored and analysed in a GIS environment such as 3DCityDB, which is an opensource 3-D geodatabase solution for modelling the physical environment based on the CityGML standard, an open data model issued by the Open Geospatial Consortium (OGC).

v. For computation of billboard dimensions using a total station, the Cosine rule can be applied instead of the join computations, given the two distances from adjacent corners and the angle between them. This was tested and the results found to be exactly the same. It would be a faster alternative compared to computing coordinates of the targeted corners then later computing the joins. Much as join computation can be considered the standard Land Survey procedure, the main objective would be determining billboard dimensions, which is not dictated by any documented procedure manual hence ultimately, so long as the result is accurate, the end justifies the means.

REFERENCES

1. Anil Can Birdal, Ugur Avdan and Tarik Turk (2017) Estimating Tree Heights with Images from an Unmanned Aerial Vehicle.
2. Arko Lucieer, DarrenTurner, Diana H. King, and Sharon A. Robinson (2014) Using an Unmanned Aerial Vehicle (UAV) to capture micro-topography of Antarctic moss beds
3. Draft Civil Aviation Unmanned Aircraft Systems Regulations 2019
4. Draft County Annual Development Plan 2020-2021
5. Francesco Mancini, Marco Dubbini, Mario Gattelli, Francesco Stecchi and Giovanni Gabbianelli (2013) Using Unmanned Aerial Vehicles (UAV) for High-Resolution Reconstruction of Topography: The Structure from Motion Approach on Coastal Environments
6. Garcia Jennifer Carrizo (2018) sustainable Outdoor Advertising in the Contemporary City
7. Juntao Lai, Tao Cheng & Guy Lansley (2017) Improved targeted outdoor advertising based on geotagged social media data, Annals of GIS, 23:4, 237-250
8. Kendra L. Johnson, Edwin Nissen, Srikanth Saripalli, J. Ramon Arrowsmith, Patrick McGarey, Katherine M. Scharer, Patrick L. Williams, Kimberly Blisniuk (2014) Rapid Mapping of Ultrafine Fault Zone Topography with Structure from Motion
9. Krysta Montgomery and Christoph Strecha (2015) Castles in the Sky
10. Mingxing Gao, Xiwei Xu, Yann Klinger, Jerome van der Woerd, and Paul Tapponnier (2017) High-resolution mapping based on an Unmanned Aerial Vehicle (UAV) to capture paleoseismic offsets along the Altyn-Tagh fault, China
11. Nairobi City Council Finance Act 2015
12. Nairobi City County Outdoor Advertising and Signage Control and Regulation Bill 2018
13. Nairobi City County Outdoor Advertising and Signage Policy (2019)
14. Nairobi City County Budget Review and Outlook paper (2019)
15. Remondino, F., Fraser, C., 2006. Digital cameras calibration methods: considerations and comparisons. IAPRS&SIS, Vol. 36(5), pp. 266-272.
16. Rodríguez, Olcese, A., M.A. & Alfaro, J. (2008): Manual De La Empresa Responsable Y Sostenible (Responsible and Sustainable Company Manual)

17. Seitz, S., Curless, B., Diebel, J., Scharstein, D., Szeliski, R., (2006). A comparison and evaluation of multi-view stereo reconstruction algorithms Vol. 1, pp. 519-528.

Web-based articles

18. Amina Wako (2019, September 19th). Crackdown on Illegally Erected Billboards Launched in Nairobi- Photos and Video. Retrieved from: https://nairobinews.nation.co.ke/hustle/crackdown-on-illegally-erected-billboards-launched-in-nairobi-photos-video [Accessed 17th January 2020]
19. Anıl Can Birdal, Uğur Avdan & Tarık Türk (2017) Estimating tree heights with images from an Unmanned Aerial Vehicle Retrieved from: https://www.tandfonline.com/doi/full/10.1080/19475705.2017.1300608 [Accessed on 15th January 2020]
20. Aznar, H. & Catalán, M. (2000). Códigos éticos de publicidad y marketing (Ethical Codes of Advertising and Marketing) Retrieved from: https://webs.ucm.es/info/especulo/numero16/et_publi.html [Accessed on 11th January 2020]
21. Derrick Koome (2019 October 17th) Drone Laws in Kenya; What to Expect in 2020. Retrieved from: https://cheswicksurveys.com/uav/drone-laws-in-kenya-what-to-expect-in-2020/ [Accessed on 13th January 2020]
22. Eunniah Mbabazi (2020 April 9th) Kenya Legalizes Drone Operations. Retrieved from: https://kenyanwallstreet.com/kenya-legalizes-drone-operations/ [Accessed on 17th April 2020]
23. Max Von Ubel (2020) 2020 Best Photogrammetric Software (Some Are Free) Retrieved from: https://all3dp.com/1/best-photogrammetry-software/ [Accessed on 12th January 2020]
24. Omulo Collins (2018 September 13th). Governor Sonko Approves Review on Nairobi's Advert Rates. Retrieved from https://www.nation.co.ke/counties/nairobi/sonko-signs-new-law-seeking-to-review-advert-rate-in-nairobi/1954174-4758024-12ypyegz/index.html [Accessed 14th January 2020]

25. Omulo Collins (2018 September 13th). Sonko Targets Sh. 2b with new law raising advertising rates. Retrieved from: https://www.businessdailyafrica.com/news/counties/Sonko-targets-Sh2bn-with-new-law/4003142-4758404-v4ujdk/index.html [accessed 15th January 2020]
26. Omulo Collins (2019). City Hall Issues Tough Advertising Rules. (March 5th) Retrieved from:https://www.nation.co.ke/counties/nairobi/City-Hall-issues-tough-advertising-rules/1954174-5010336-xl1y1fz/index.html [accessed 15th January 2020]
27. Paul R. Wolf (2000) Elements of Photogrammetry Third Edition. Published by American Society for Photogrammetry & Remote Sensing. Retrieved from: https://www.pcigeomatics.com/geomatica-help/COMMON/concepts/ExteriorOrientation_explainEO.html [Accessed on 17th January 2020]
28. Tanguay Photo Mag (2019) Aerial Photography. Retrieved from: https://www.tanguayphotomag.biz/aerial-photography/creating-stereomodels-with-aerial-triangulation-by-bundleblock-adjustment.html [Accessed on 20th January 2020]
29. Theia-sfm.org, (2020). Structure from Motion (SfM) — Theia Vision Library. [online] Retrieved from: http://www.theia-sfm.org/sfm.html [Accessed 16th January 2020]

APPENDICES

Appendix A: Survey Computations for Billboard 1

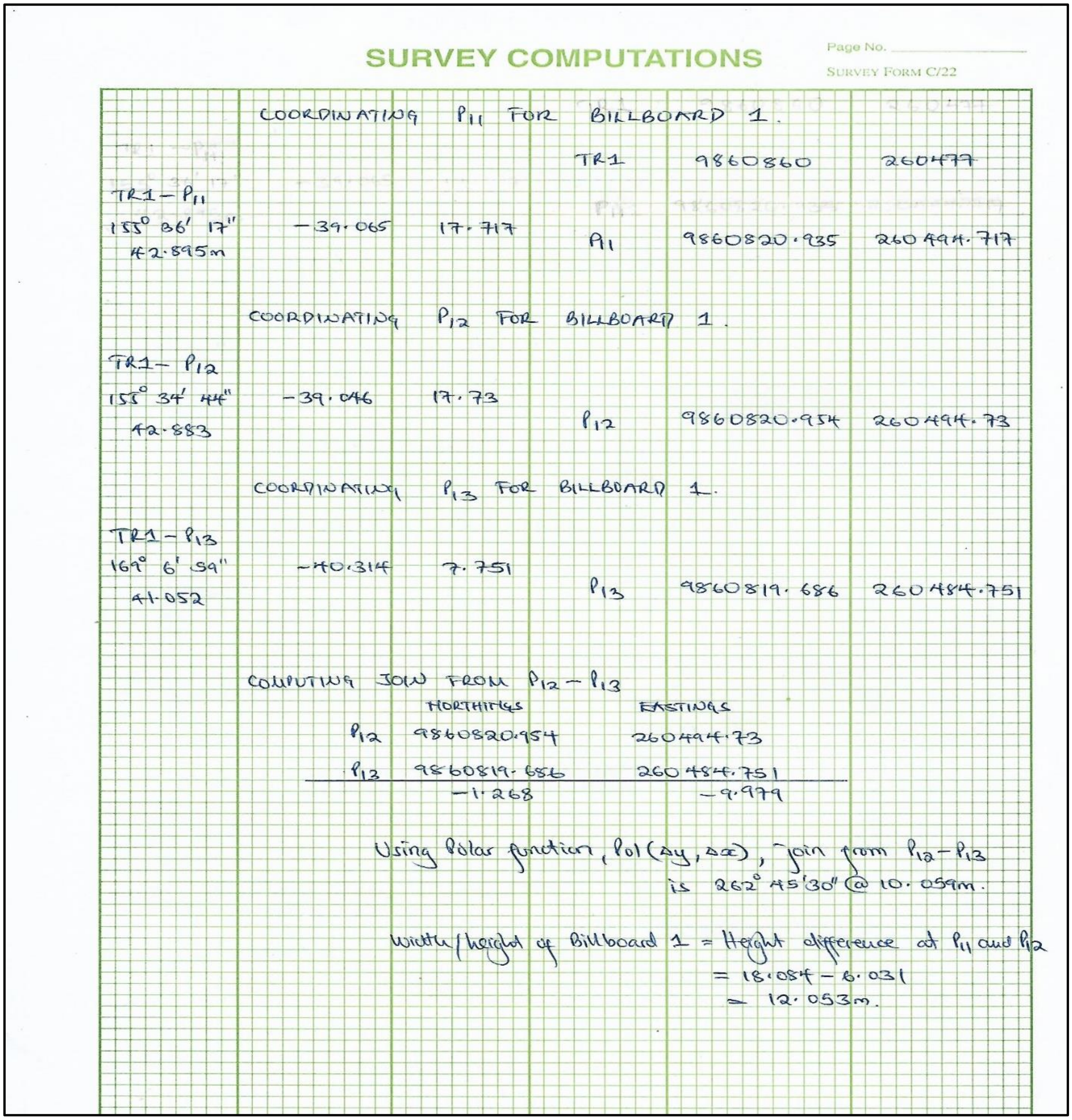

SURVEY COMPUTATIONS

Page No.

SURVEY FORM C/22

COORDINATING P_{11} FOR BILLBOARD 1.

			TR1	9860860	260477
TR1 – P_{11} 155° 36′ 17″ 42.895m	–39.065	17.717	P_{11}	9860820.935	260494.717

COORDINATING P_{12} FOR BILLBOARD 1.

TR1 – P_{12} 155° 34′ 44″ 42.883	–39.046	17.73	P_{12}	9860820.954	260494.73

COORDINATING P_{13} FOR BILLBOARD 1.

TR1 – P_{13} 169° 6′ 59″ 41.052	–40.314	7.751	P_{13}	9860819.686	260484.751

COMPUTING JOIN FROM P_{12} – P_{13}

	NORTHINGS	EASTINGS
P_{12}	9860820.954	260494.73
P_{13}	9860819.686	260484.751
	–1.268	–9.979

Using Polar function, Pol(Δy, Δx), join from P_{12} – P_{13} is 262° 45′ 30″ @ 10.059m.

Width/height of Billboard 1 = Height difference at P_{11} and P_{12}
= 18.084 – 6.031
= 12.053m.

Appendix B: Survey Computations for Billboard 2

SURVEY COMPUTATIONS Page No. ______

SURVEY FORM C/22

COORDINATING P_{21} FOR BILLBOARD 2.

			TR1	9860860	260477
TR1 – P_{21} 149° 25' 41" 114.245m	-98.367	58.109	P_{21}	9860761.633	260535.109

COORDINATING P_{22} FOR BILLBOARD 2.

TR1 – P_{22} 149° 24' 58" 114.607	-98.663	58.312	P_{22}	9860761.337	260535.312

COORDINATING P_{23} FOR BILLBOARD 2

TR1 – P_{23} 154° 10' 22" 110.958	-99.875	48.34	P_{23}	9860760.125	260525.34

COMPUTING JOIN FROM P_{22} – P_{23}

	NORTHINGS	EASTINGS
P_{22}	9860761.337	260535.312
P_{23}	9860760.125	260525.34
	– 1.212	– 9.972.

Using Polar function, Pol (Δy, Δx), join from P_{22} – P_{23} is 263° 4' 13" @ 10.045 m.

Width/height of Billboard 2 = Height difference @ P_{21} and P_{22}

= 20.338 – 8.281

= 12.057m.

Appendix C: Survey Computations for Billboard 3

SURVEY COMPUTATIONS

Page No. ____

SURVEY FORM C/22

COORDINATING P_{31} FOR BILLBOARD 3.

TR1. 9860860 260477

TR1 – P_{31}

111° 57' 03" -41.477 102.914

110.958m P_{31} 9860818.52 260579.914

COORDINATING P_{32} FOR BILLBOARD 3.

TR1 – P_{32}

111° 51' 02" -60.389 150.597

165.254 P_{32} 9860799.611 260627.597

COORDINATING P_{33} FOR BILLBOARD 3.

TR1 – P_{33}

116° 48' 27" -72.049 142.587

159.756 P_{33} 9860787.951 260619.587

COMPUTING JOIN FROM P_{32} – P_{33}

	NORTHINGS	EASTINGS
P_{32}	9860799.611	260627.597
P_{33}	9860787.951	260619.587
	-11.66	-8.01

Using Polar function, Pol (Δy, Δx), join from P_{32} – P_{33} is 214° 29' 15" @ 14.146m

Width/height of Billboard 3 = Height difference @ P_{31} and P_{32}

= 17.893 – 7.295

= 10.598m.